scientific reports

Check for updates

OPEN

A new species of the mud terrapin *Pelusios* offers insights into early hominin habitats at the Pliocene Hadar Formation of Ethiopia

Brent Adrian✉, Christopher J. Campisano, Kaye E. Reed & Denise F. Su

A novel extinct species of mud terrapin *Pelusios awashi* sp. nov. is described from the Hadar Formation in Ethiopia. Referred specimens include articulated and isolated specimens from multiple individuals that represent most elements of the shell and a holotype skull, which is the first known from the fossil record of *Pelusios*. The new species is distinct from extant *Pelusios* species by a unique combination of: a broad maxilla with an extensive triturating surface, a neural series reaching the suprapygal, and moderately convex lateral hypoplastral margins. *Pelusios* is unique among pleurodires for its kinetic plastral hinge at the hyo-mesoplastral junction, and the angled hinge of the new species demonstrates a plesiomorphic condition. Specimens found at the "First Family" locality (A.L. 333) in the Denen Dora Member suggest overlap between hominins and terrapins in habitats with aquatic resources. Crocodile bite marks denote likely chelonivory by *Crocodylus* and may indicate increased predation risk for sympatric hominins. The paleoecology of *Pelusios awashi* sp. nov. probably resembled that of *P. sinuatus*, consistent with phylogenetic and climatic niche conservatism in modern turtles. However, the broader maxilla of the new species suggests a more durophagous diet.

Keywords Pleurodire, Pelomedusidae, Neogene, Crocodile predation, Durophagy, Africa

While turtle fossils are found at many Plio-Pleistocene hominin sites, they are not well understood due to common logistical constraints on their storage and collection and frequently fragmentary preservation, which can confound taxonomic identification. Yet, they represent specific environmental requirements that can inform us of the ecological conditions in which hominins evolved. Here, we describe a new species of mud terrapin – *Pelusios* – from Hadar, Ethiopia, one of the most important hominin sites for understanding early human evolution[1].

Pelusios[2] is a genus of side-necked turtles[3–8] (Pleurodira) with seventeen extant species inhabiting sub-Saharan Africa, Madagascar, Príncipe, São Tomé, and the Seychelles, including introductions in the Lesser Antilles[8–11]. *Pelusios* is the sister taxon to *Pelomedusa*[2], the African helmeted turtle, and the two comprise Pelomedusidae[12]. Fossil evidence suggests their divergence in or before the Early Miocene[13]. Like *Pelusios*, *Pelomedusa* is widespread in Africa and comprises at least ten species[12,14]. Pelomedusidae, along with the South American-Malagasy Podocnemididae, are the last surviving pelomedusoid turtles[8,15]. During the Cretaceous and Paleogene, Pelomedusoides were diverse across most landmasses except Central Asia, Australia, and Antarctica, but Pelomedusidae is a strictly African radiation[16,17].

Three fossil *Pelusios* species are known, including: the Early Miocene (~ 23.0–16.0 Ma) *Pelusios rusingae*[18] from Rusinga Island (Kenya), represented by a partial carapace and plastron[19]; *Pelusios dewitzianus*[20], known by fragments from Pliocene deposits at Wadi El Natrun (Egypt)[18]; and a partial plastron and carapace of *Pelusios rudolphi*[21] from Lower Pleistocene strata in the Omo River Basin (Ethiopia)[12,16]. A fossilized shell attributed to the extant species *Pelusios sinuatus* is also known from Pleistocene Bed I at Oldupai (formerly Olduvai) Gorge (Tanzania)[18,22,23]. The evolutionary history of *Pelusios* reflects complex biogeographic, ecological, and genetic dynamics among its numerous species[11]. Weak genetic divergence, particularly among continental African, Malagasy, and Seychellois populations suggests recent, rapid dispersal, sometimes aided by human transport (e.g., as a food source)[24]. However, molecular analyses have clarified some phylogenetic relationships and highlighted adaptations to various freshwater habitats[9,24].

Institute of Human Origins and School of Human Evolution and Social Change, Arizona State University, Tempe, AZ 85287, USA. ✉email: badrian@asu.edu

All *Pelusios* species are highly aquatic and inhabit freshwater environments from savannas to rainforests[6,8]. These mud terrapins are primarily carnivorous benthic foragers that feed on invertebrates, fish, and amphibians in lakes, marshes, swamps, and ephemeral waterways[25,26]. Some species can tolerate brackish waters and others are known to aestivate in the dry season[8]. Most species range from 20 to 30 centimeters (cm) in carapace length and females are generally larger than males[25]. The smallest species, *Pelusios nanus*, is approximately 12 cm long and the largest, *Pelusios sinuatus*, can exceed 46 cm[27]. Adult female *Pelusios sinuatus* have a typical carapace length of approximately 40 cm compared to about 35 cm in males[25]. All *Pelusios* species besides *Pelusios broadleyi*[28] possess a functional hinge between the hyo- and mesoplastra, allowing partial or full shell closure, a unique adaptation among pleurodiran turtles[8,29]. Hinge mobility reduces predation risk and is complemented by other defensive traits like sharp claws, strong jaws, and musk glands[25,29,30].

Geological setting

Fossil material in this study was recovered from the Pliocene Hadar Formation (Fm.) (~ 3.8 – 2.9 Ma) in the Afar Depression of Ethiopia[1,31–33] (Fig. 1A-B). Located along the southern edge of the Afar Triangle, the Hadar Fm. is part of eastern Africa's Great Rift Valley[1,34]. The formation is divided by laterally extensive dated tuff horizons into the Basal (~ 3.8–3.42 Ma), Sidi Hakoma (~ 3.42–3.26 Ma), Denen Dora (~ 3.26 – 3.2 Ma), and Kada Hadar (~ 3.2– 2.9 Ma) Members, which are further divided into submembers[1,31,33,35] (Fig. 1C). Hadar deposits have produced one of the most taxonomically diverse and abundant mid-Pliocene faunas in eastern Africa, and its mammalian taxa have been studied extensively for over four decades[1,36]. Importantly, it has yielded the largest sample of *Australopithecus afarensis*, a key early hominin species hypothesized to be ancestral to our own genus *Homo*[36–43]. In contrast, the herpetofauna from Hadar remain understudied, aside from the discovery of preserved turtle eggs[37]. Additional information regarding geological setting is provided in the Supplemental Information.

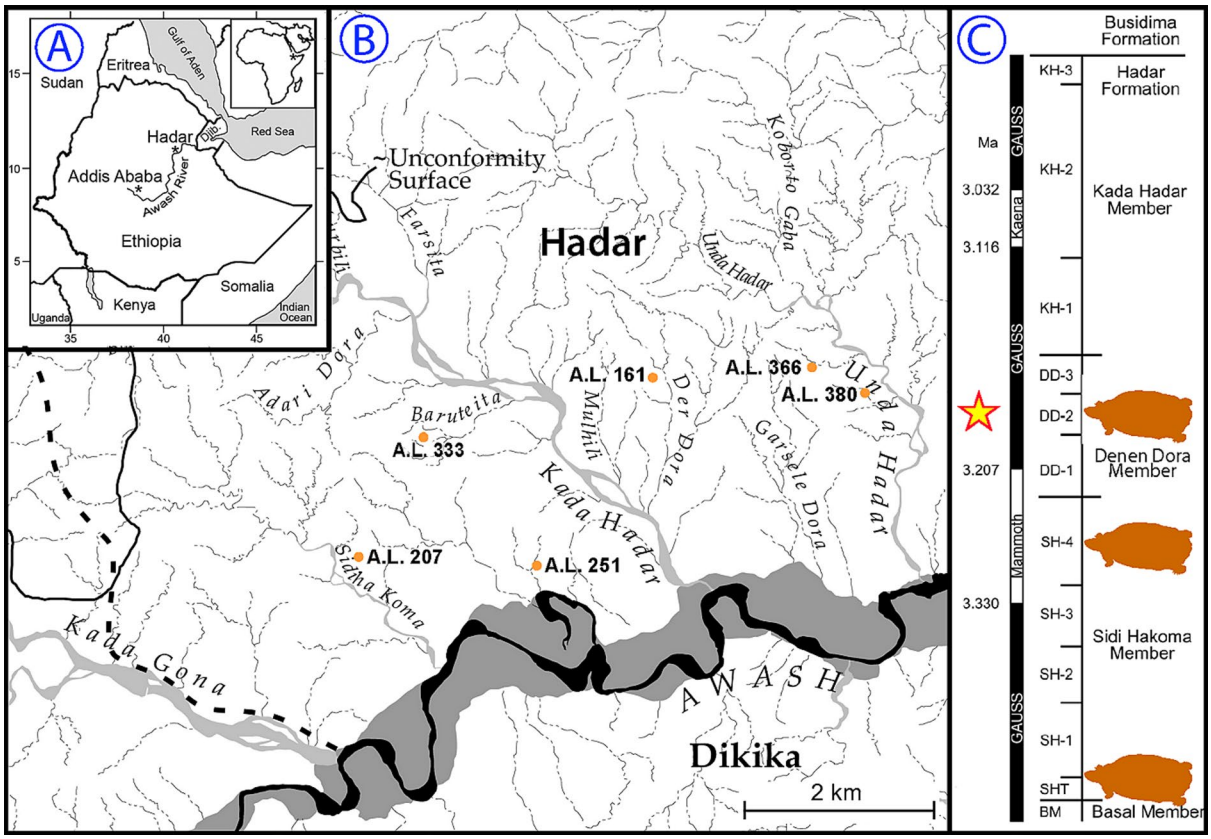

Fig. 1. Location and geologic setting of the Hadar Formation. (**A**) Regional and continental map of the Hadar paleoanthropological site, (**B**) drainage map, and (**C**) composite stratigraphic section. Dashed lines show approximate boundaries with adjacent research areas. Orange dots in (**B**) indicate Hadar localities where *Pelusios awashi* sp nov. has been found. Yellow star indicates A.L. 333, the "First Family" locality. Orange turtle silhouettes indicate approximate stratigraphic position of remains of the new species and are utilized in concordance with Public Domain Mark 1.0 from http://www.phylopic.com (uploaded 2023 by Luca Leicht). Figure created with Adobe Creative Cloud[122].

Results

Systematic paleontology

Pleurodira[44].

Pelomedusoides[45].

Pelomedusidae[46]

Pelusios[2] .

Pelusios awashi sp. nov.

Figures 2, 3, 4, 5, 6, 7, 8 and 9.

Holotype: A.L. 207 – 15, a partial cranium.

Type locality and horizon: Pliocene, Denen Dora Member, DD-2 submember, Hadar Formation[31], Ethiopia (Fig. 1C). Exact locality data are on file at the National Museum of Ethiopia in Addis Ababa.

Etymology: The specific epithet refers to the Awash River, a major Ethiopian waterway renowned for its association with important fossil deposits, which have yielded some of the most significant known early hominin remains.

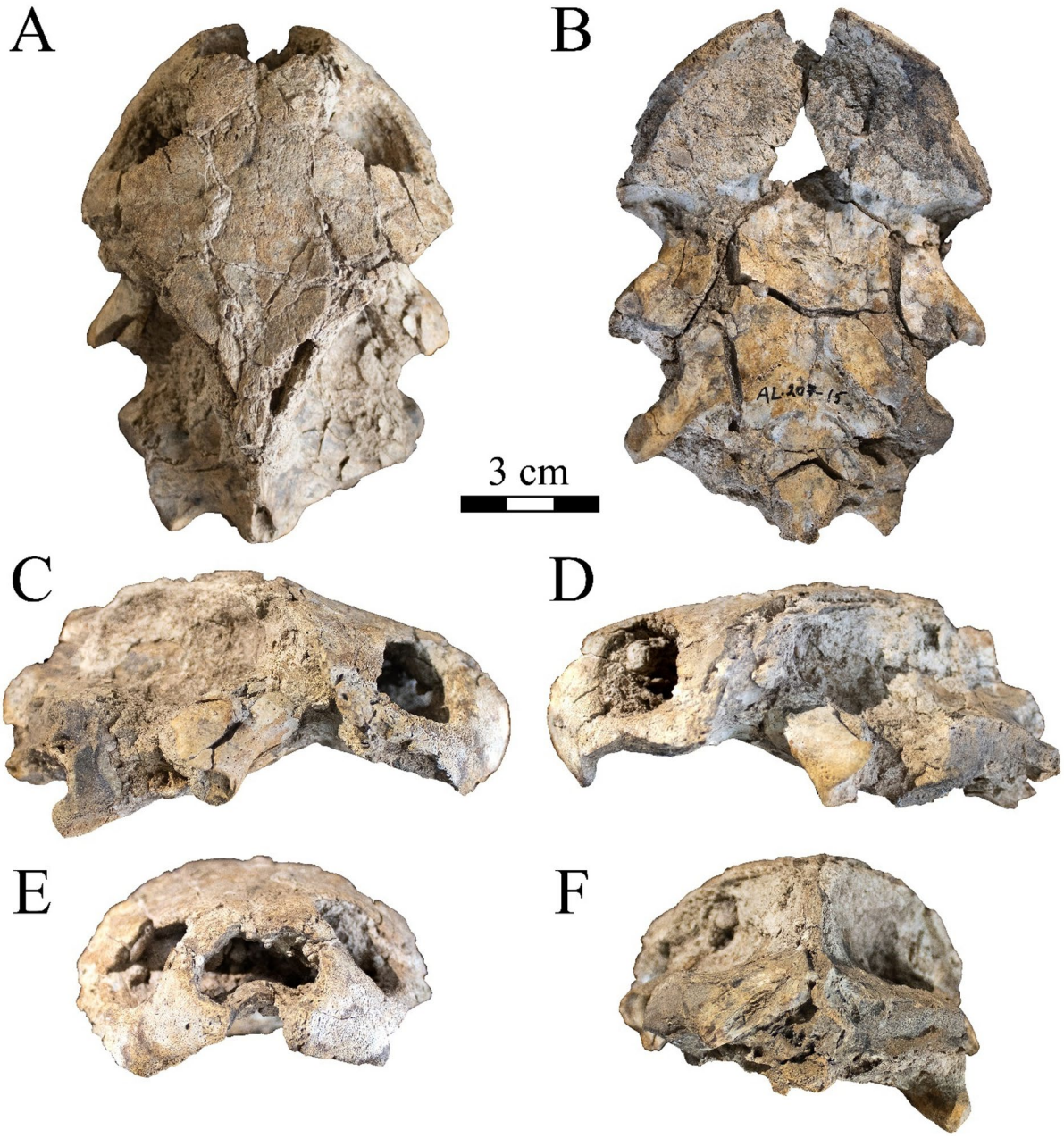

Fig. 2. Photographs of A.L. 207 – 15, a partial skull and holotype of *Pelusios awashi sp*. nov. in (**A**) dorsal, (**B**) ventral, (**C**) right lateral, (**D**) left lateral, (**E**) anterior, and (**F**) posterior views. Figure created with Adobe Creative Cloud[122].

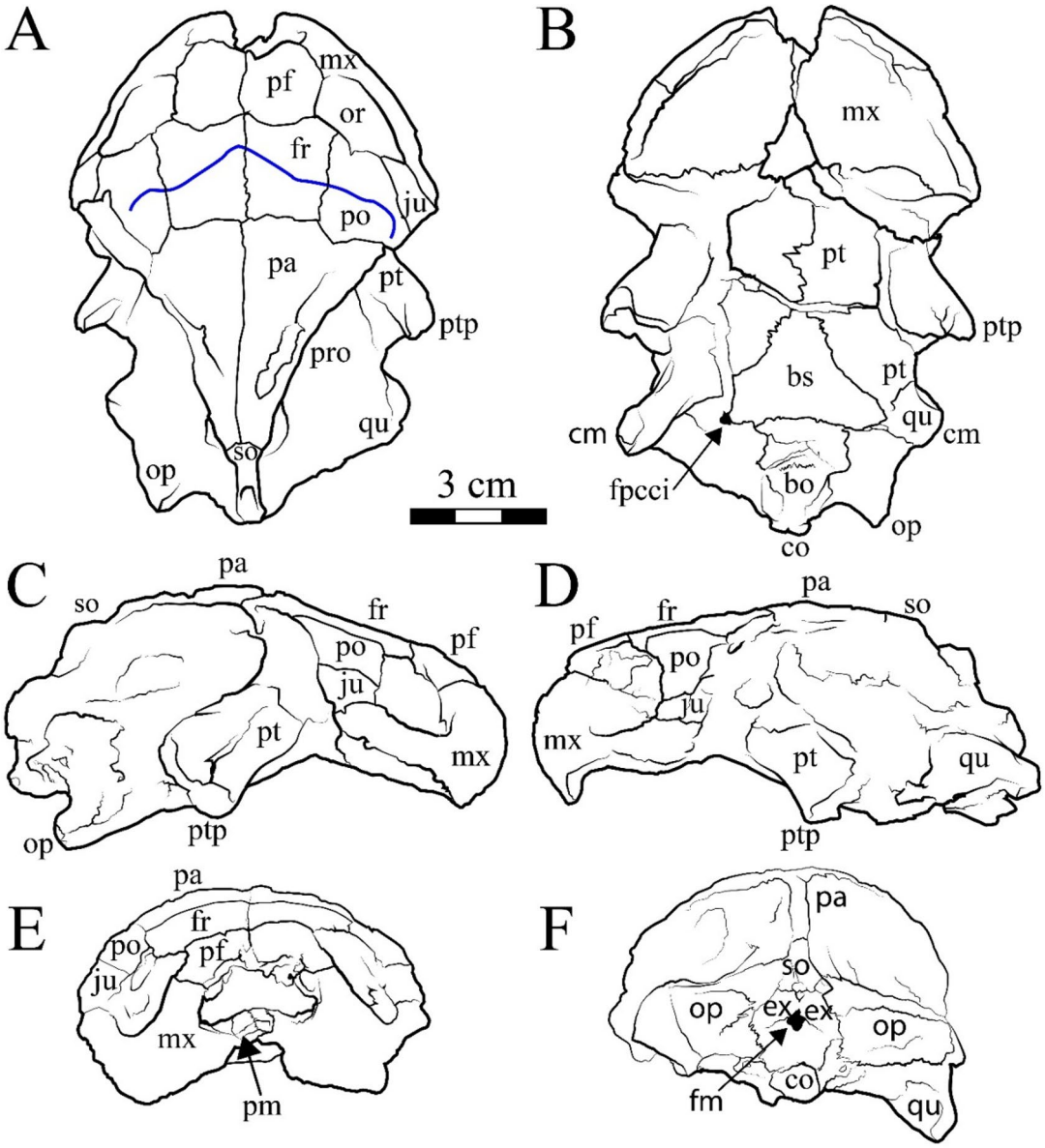

Fig. 3. Line drawings of A.L. 207 – 15, a partial skull and holotype of *Pelusios awashi sp*. nov. in (**A**) dorsal, (**B**) ventral, (**C**) right lateral, (**D**) left lateral, (**E**) anterior, and (**F**) posterior views. Blue line indicates sulcus between supraocular and frontal head scales[27]. Abbreviations: bo = basioccipital, bs = basisphenoid, cm = condylus mandibularis, co = condylus occipitalis, ex = exoccipital, fpcci = foramen posterius canalis carotici interni, fr = frontal, ju = jugal, mx = maxilla, op = opisthotic, or = orbit, p.a. = parietal, pal = palatine, pf = prefrontal, pm = premaxilla, po = postorbital, pro = prootic, pt = pterygoid, ptp = processus trochlearis pterygoidei, qu = quadrate, so = supraoccipital. Figure created with Adobe Creative Cloud[122].

Referred material: See Table 1. A.L. 251 – 39, bilateral hypoplastra including right inguinal buttress; A.L. 380-3, partial carapace including costals, posterior peripherals, neurals, pygal and suprapygal; A.L. 161 – 26, right meso-, hypo-, and xiphiplastron; A.L. 366-4, partial right plastron including meso-, hypo-, xiphi-, epi-, and entoplastron; A.L. 207 – 15, partial cranium; A.L. 333w-510, right xiphiplastron; A.L. 333w-511, cf. juvenile right xiphiplastron; A.L. 333w-512, costal fragment with crocodile bite marks; A.L. 333w-513, cf. juvenile right epiplastron; A.L. 333w-514, right peripheral 11; A.L. 2137-1a, complete right epiplastron, partial left epiplastron, partial right hyoplastron, and partial entoplastron; A.L. 2137-1b, pygal; A.L. 2138-1a, right costal 8, A.L. 2138-1b, left xiphiplastron.

Diagnosis: The holotype skull A.L. 207 – 15 (Fig. 2) is recognized as belonging to Pleurodira based on the anterior location of the condylus mandibularis base relative to the basioccipital-basisphenoid suture, and the processus trochlearis pterygoidei is also a distinctively pleurodiran trait. The skull is attributed to Pelomedusoides by absent parietal-squamosal contact and nasals, as well as medial contact between prefrontals. It represents Pelomedusidae by exoccipitals that exclusively form the condylus occipitalis. The parietals are consistent with

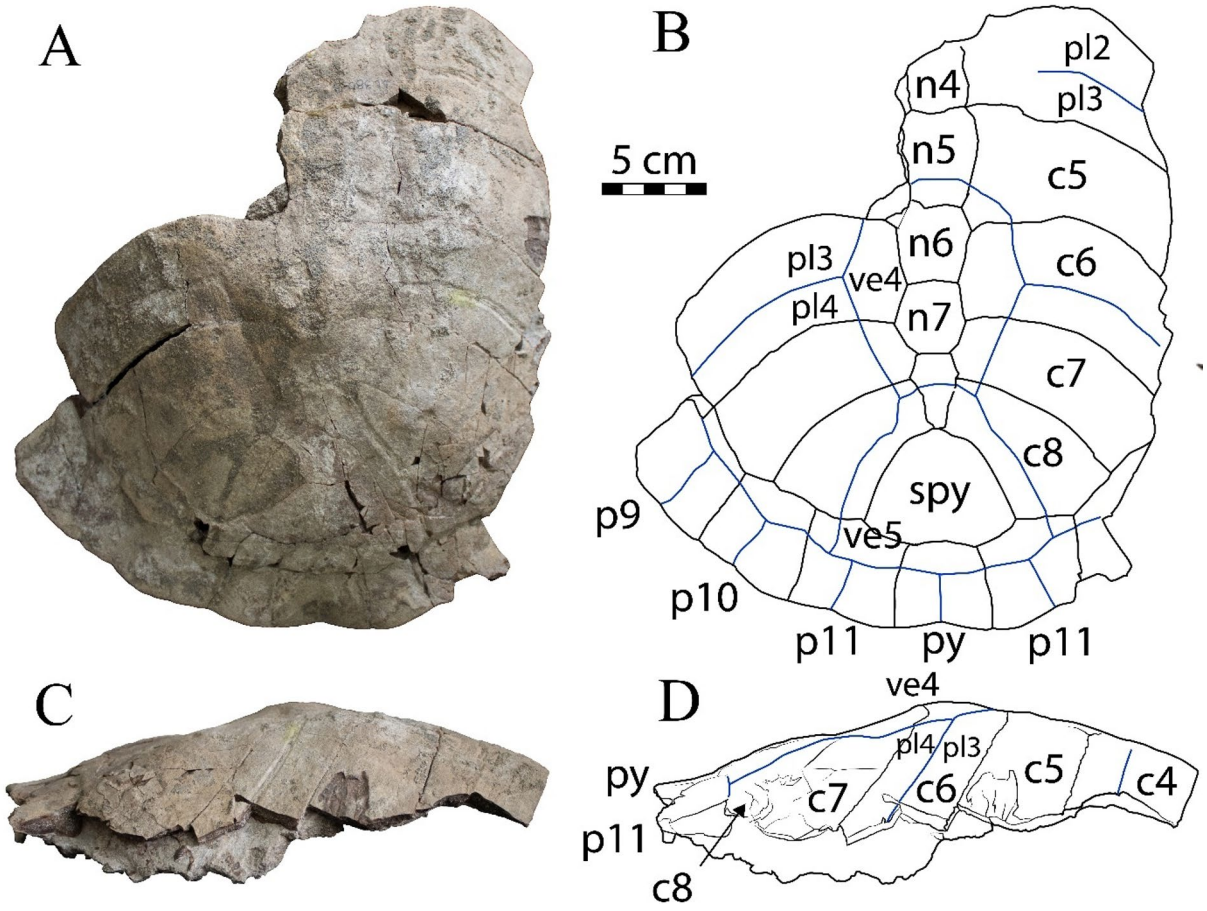

Fig. 4. A.L. 380-3, a partial carapace of *Pelusios awashi* sp. nov. (**A**) Dorsal photograph, (**B**) dorsal drawing, (**C**) right lateral photograph, (**D**) right lateral drawing. Abbreviations: c = costal, n = neural, p = peripheral, pl = pleural scale, py = pygal, spy = suprapygal, ve = vertebral scale. Blue lines indicate sulci. Figure created with Adobe Creative Cloud[122].

the plesiomorphic emarginated condition seen in pelomedusids, as opposed to the more extensively roofed condition of bothremydids (e.g., *Bothremys*) and podocnemidids (e.g., *Dacquemys*). In the new species, the exclusion of the basioccipital from the condylus occipitalis by the exoccipitals differs from the plesiomorphic condition in some other pleurodires (i.e., podocnemidids, euraxemydids, chelids, Kurmademydini)[17]. The basioccipital is typically excepted from the occipital condyle in pelomedusids but contributes to it in *Pelusios sinuatus* and *P. niger* (Gaffney, 2006). The holotype skull is distinguished from that of *Pelomedusa* by its larger size and lesser degree of temporal embayment, and size also differentiates the skull from all congenerics except *Pelusios sinuatus*. In comparison with the latter taxon, the skull of *Pelusios awashi* sp. nov. has a broader maxilla and triturating surface and a wider interorbital region. The skull of the new taxon is distinguished from that of *Mokelemys mbembe*[47] by lacking: an interorbital longitudinal depression, and an accessory ridge on the maxillary palatal surface[47]. The shell of *Pelusios awashi* sp. nov. can be differentiated from that of *M. mbembe* by having eight neurals that reach the suprapygal. The shell of the new species (Figs. 2, 3, 4, 5 and 6) is distinguished from all extinct and modern congenerics by a unique combination of the following traits: a neural series that reaches the suprapygal (Fig. 4); mesoplastra with midline contact and anterior edges forming an angle (Figs. 7 and 9); and moderately convex lateral hypoplastral margins posterior to the abdominal-femoral sulcus (Fig. 7A-L). *Pelusios awashi* sp. nov. is distinct from *Kenyemys*[48] based on: the lack of a narrow keel along the neural series; number of neurals; no contact between bilateral posterior costals at the midline; gular scale overlap onto the entoplastron; shape of the anterior plastral lobe margin; and the complete separation of extragular scales at the midline by the gular scale[48].

Description:

Skull. The holotype skull A.L. 207 – 15 of *Pelusios awashi* sp. nov. is well preserved and undistorted, particularly in the dorsal aspect of the cranium, which retains sulci of frontal and supraocular cranial scales on the skull roof[27,49] (Figs. 2 and 3). Most of the missing areas of bone are confined to parts of the skull that are laterally situated and posterior to the facial region, including the cavum tympani, fossae temporalis superior, and antrum postoticum. The orbits are subrounded and slightly compressed dorsal-ventrally, facing more anterolaterally than dorsally (Fig. 3A, C-E). The supratemporal fossa is partially infilled with sandy matrix on both sides. The prefrontals form the most anterior element of the skull roof and are approximately as wide as long and contact

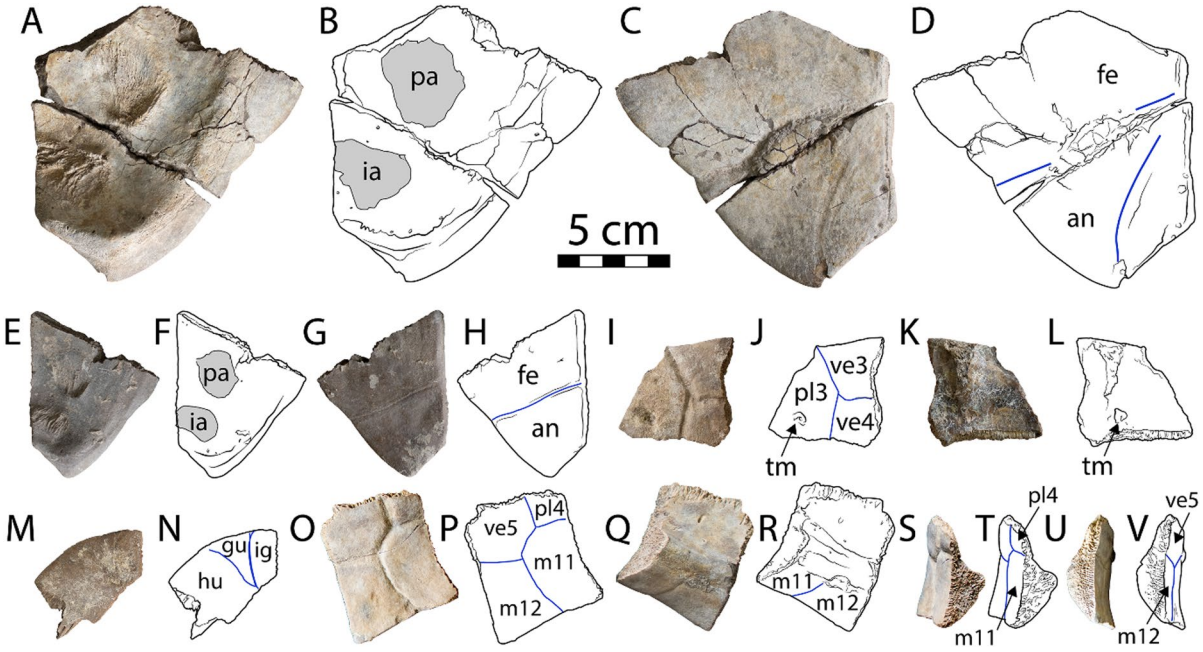

Fig. 5. Isolated elements of *Pelusios awashi* sp. nov. from the A.L. 333w "First Family" locality. (**A**) Dorsal photograph, (**B**) dorsal drawing, (**C**) ventral photograph, and (**D**) ventral drawing of right xiphiplastron A.L. 333w-510. (**E**) Dorsal photograph, (**F**) dorsal drawing, (**G**) ventral photograph, and (**H**) ventral drawing of cf. juvenile right xiphiplastron A.L. 333w-511. (**I**) Dorsal photograph, (**J**) dorsal drawing, (**K**) ventral photograph, and (**L**) ventral drawing of medial (cf. fifth) costal fragment A.L. 333w-512 with crocodile tooth marks. (**M**) Ventral photograph and (**N**) ventral drawing of right epiplastron A.L. 333w-513. (**O**) Dorsal photograph, (**P**) dorsal drawing, (**Q**) ventral photograph, (**R**) ventral drawing, (**S**) anterior photograph, (**T**) anterior drawing, (**U**) posterior photograph and (**V**) posterior drawing of right peripheral 11 A.L. 333w-514. Solid blue lines represent sulci. Figure created with Adobe Creative Cloud[122]. Abbreviations: an = anal scale, fe = femoral scale, gu = gular scale; hu = humeral scale, i.a. = ischial articulation, m = marginal scale, p.a. = pelvic articulation, pl = pleural scale, tm = tooth mark; ve = vertebral scale.

each other at the midline anterior to the frontals. The nasals are absent, as in other pleurodires[17]. The frontals form the posterior portion of the interorbital roof and the orbital margins (Fig. 3A, C-E). They are slightly longer than wide in A.L. 207 – 15 and wider anteriorly than posteriorly. The anterior edge of each frontal is concave posteriorly in its contact with the prefrontals.

The dorsal plate of the parietals in A.L. 207 – 15 is distinctly emarginate. Each parietal bone is approximately triangular and longer than wide with its long aspect oriented posteriorly (Fig. 3A, C-F). The posterolateral margins of the parietals and postorbitals are slightly concave laterally, forming the anterior margin of the temporal emargination. Each jugal forms a flat lateral plate along the posterior margin of the orbit that is longer than wide. The quadratojugals and squamosals are missing in A.L. 207 – 15. The postorbital bones are flat, dorsolateral plates of the temporal roof and contribute to the dorsal and posterior margins of the orbit and the anterior margin of the temporal emargination, posterior to the jugals (Fig. 3A, C-E). The premaxilla is mostly missing, but it probably occupied an empty space at the midline of the anterior end of the rostrum. A small portion of the element remains along the midline of the anterior floor of the fossa nasalis, accentuating the already considerable shortness of the face of *Pelusios awashi*, sp. nov. (Fig. 3E).

In ventral view, the maxillae are well preserved but missing their ventralmost edges posteriorly on both sides. This damage makes the maxillae appear shorter dorsoventrally when viewed laterally and gives it a hook-like appearance (Fig. 3C-D). The maxillae provide a distinctively wide and round appearance for the face and palate when viewed dorsally or ventrally (Fig. 3A-B). The vomer is absent in A.L. 207 – 15 as in other pelomedusids[17]. On the ventral side of A.L. 207 – 15, the palatines contact each other in the space between the maxillae and have collapsed toward the interior of the skull at their anterior ends. The quadrate is large and complex in pleurodires, and it forms the middle and outer ear laterally, as well as structures associated with the cranioquadrate space medially[17,50]. The quadrate is largely missing in A.L. 207 – 15, and the cranioquadrate space is partially preserved (Figs. 2 and 3). The quadrate typically contributes substantially to the cavum tympani, but the latter is not preserved. The preserved portions of the quadrates of A.L. 207 – 15 are generally located posterior to the prootics in dorsal view, but superficial damage obscures the precise location of sutures (Fig. 3A). These portions of the quadrate project laterally and slightly posteriorly from the skull to form the medial part of the right condylus mandibularis, while the lateral portion is missing (Fig. 3A-C, F).

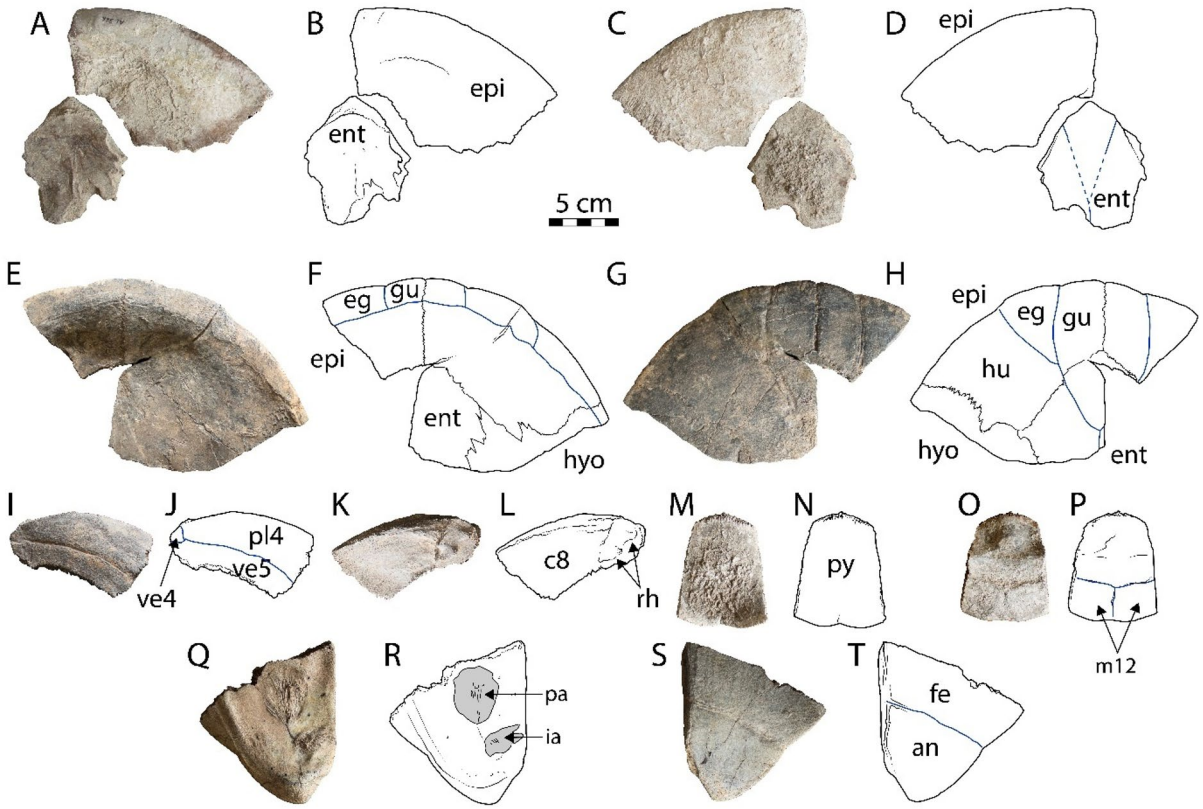

Fig. 6. Additional isolated elements of *Pelusios awashi* sp. nov. (**A**) Dorsal photo, (**B**) dorsal drawing, (**C**) ventral photo and (**D**) ventral drawing of entoplastron and right epiplastron from A.L. 366-4. (**E**) Dorsal photograph, (**F**) dorsal drawing, (**G**) ventral photograph and (**H**) ventral drawing of partial anterior plastral lobe A.L. 2137-1a. (**I**) dorsal photograph, (**J**) dorsal drawing, (**K**) ventral photograph and (**L**) ventral drawing of right costal 8 A.L. 2138-1a. (**M**) Dorsal photograph, (**N**) dorsal drawing, (**O**) ventral photograph and (**P**) ventral drawing of pygal A.L. 2137-1b. (**Q**) Dorsal photograph, (**R**) dorsal drawing, (**S**) ventral photograph and (**T**) ventral drawing of left xiphiplastron A.L. 2138-b. Figure created with Adobe Creative Cloud[122]. Abbreviations: an = anal scale, c = costal, eg = extragular scale, ent = entoplastron, epi = epiplastron, fe = femoral scale, gu = gular scale; hyo = hyoplastron, m = marginal scale, py = pygal. Solid blue lines represent sulci, and dotted blue lines represent estimated path of sulci.

The pterygoids of A.L. 207 − 15 are horizontally oriented, and the prominent lateral processus trochlearis pterygoidei is curved distally with a thin ventrolateral flange (Fig. 3A-D). The processus trochlearis pterygoidei is an important pleurodiran synapomorphy that is preserved on both sides of A.L. 207 − 15, forming prominent trochleae for the main jaw adductor tendons[17]. The processus trochlearis pterygoidei curls medially and dorsally toward the sulcus palatinopterygoideus, which forms a medial trough-like space. The epipterygoid is absent in A.L. 207 − 15, which is another pleurodiran synapomorphy[5,17]. A short dorsal segment of the supraoccipital is preserved in A.L. 207 − 15 at the posterior end of the parietals, and it forms the base of the crista supraoccipitalis, which is otherwise missing (Fig. 3A, C-D, F). In posterior view, the supraoccipital is located dorsal to the exoccipitals and foramen magnum, and it does not contribute to the latter feature (Fig. 3F). Its ventral extent in this specimen is otherwise poorly defined.

The exoccipitals are located at the back of the skull posterior to the basioccipital along the midline (Fig. 3F). They contribute to the sides and floor of the posterior braincase in A.L. 207 − 15, as in other pleurodires[17]. In A.L. 207 − 15, the exoccipital forms the condylus occipitalis to the exclusion of the more anteriorly located basioccipital but is not exposed on the damaged ventral aspect of the condyle (Fig. 3B). In ventral view, the basioccipital of A.L. 207 − 15 is located between the basisphenoid anteriorly and the exoccipitals posteriorly and dorsally. Paired processes project posterolaterally from the midline, forming a triangular tuberculum basioccipitale (Fig. 3B), which serves as a bilaterally short and wide attachment site for vertebral connective tissue[17]. In A.L. 207 − 15, the basioccipital does not contribute to the foramen magnum or condylus occipitalis. The prootic is located between the pterygoid anterolaterally and the quadrate posterolaterally, but their sutural contacts are unclear due to poor preservation (Fig. 3A). The area surrounding the prootic is damaged ventrally but likely contributes to the foramen posterius canalis carotici interni. The opisthotics of A.L. 207 − 15 are partially present although their extent is difficult to assess. A large triangular process projects posterolaterally from the left side (Fig. 3A-C, F). The opisthotic contacts at least the quadrate anterolaterally, prootic anteriorly, and basioccipital medially. Further bony contacts cannot be assessed due to damage and obscured sutures.

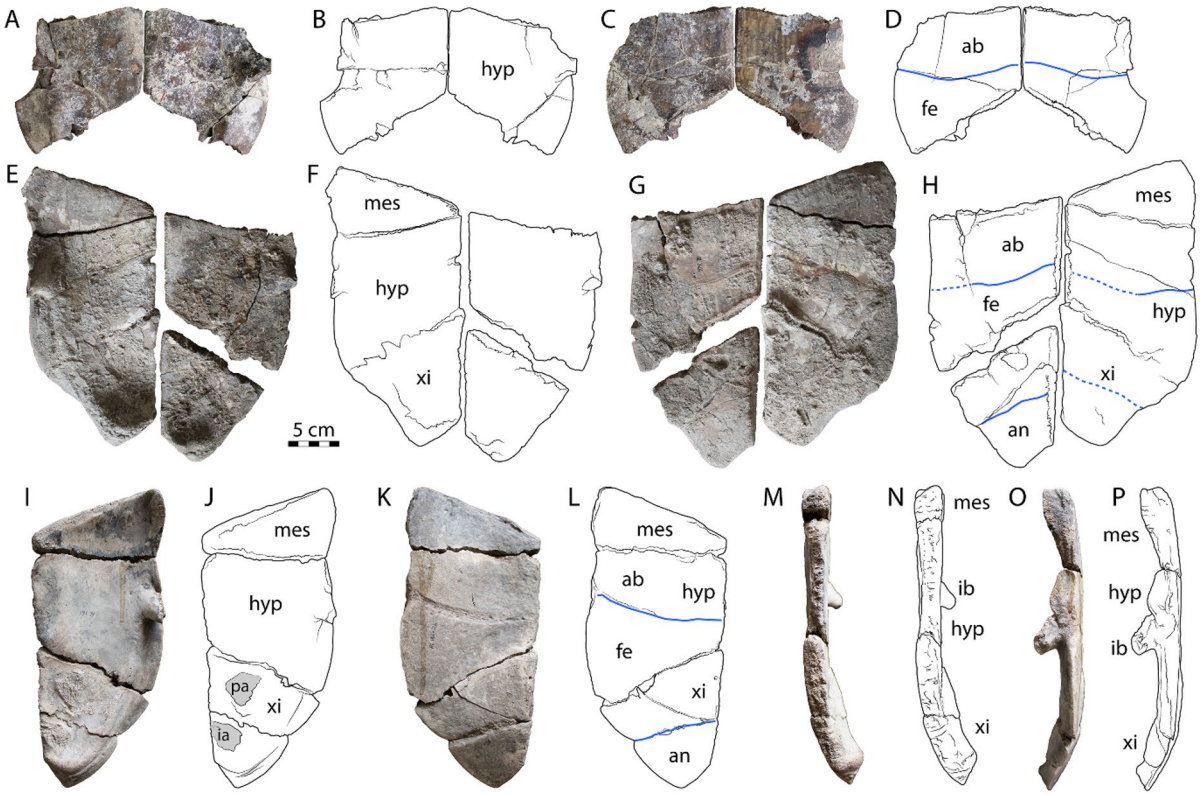

Fig. 7. Partial plastra of *Pelusios awashi* sp. nov. (**A**) Dorsal photograph, (**B**) dorsal drawing, (**C**) ventral photograph and (**D**) ventral drawing of bilateral hypoplastra A.L. 251 – 39. (**E**) Dorsal photograph, (**F**) dorsal drawing, (**G**) ventral photograph and (**H**) ventral drawing of bilateral hypo- and xiphiplastra and left mesoplastron of A.L. 366-4. (**I**) Dorsal photograph, (**J**) dorsal drawing, (**K**) ventral photograph and (**L**) ventral drawing of right meso-, hypo-, and xiphiplastron A.L. 161 – 26. Figure created with Adobe Creative Cloud[122]. Abbreviations: ab = abdominal scale, an = anal scale, fe = femoral scale, hyp = hypoplastron, i.a. = ischial articulation, ib = inguinal buttress, mes = mesoplastron, p.a. = pubic articulation, xi = xiphiplastron. Solid blue lines represent sulci, and dotted blue lines represent estimated path of sulci.

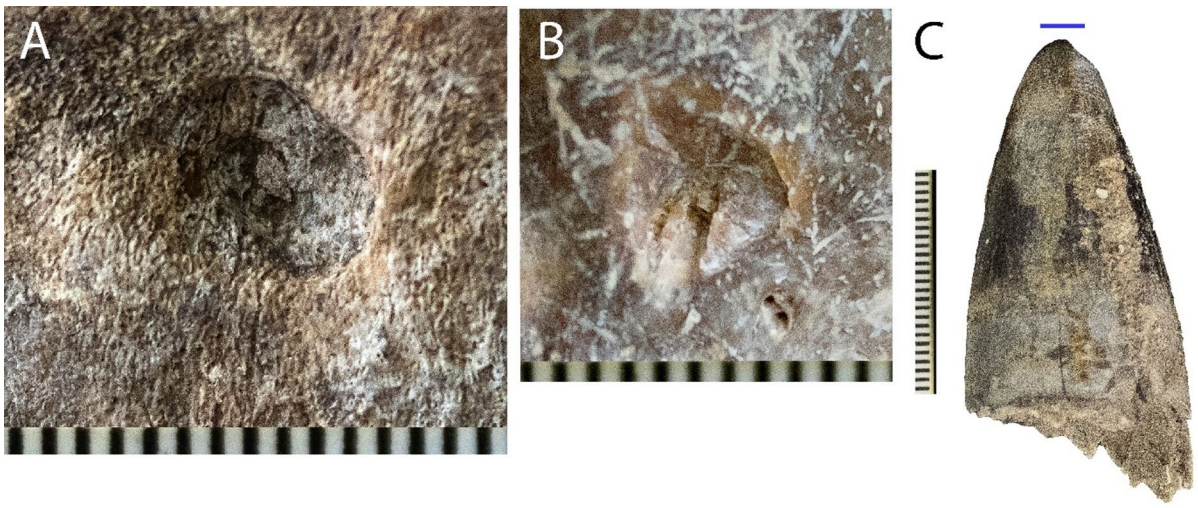

Fig. 8. Probable crocodile tooth marks on medial likely fifth costal fragment from A.L. 333w-512. (**A**) dorsal surface, (**B**) ventral surface, (**C**) A.L. 834-1, a representative large crocodile (cf. *Crocodylus*) tooth from the Hadar Fm. A and B are scaled equally, different from C. Horizontal blue line is 5 mm.

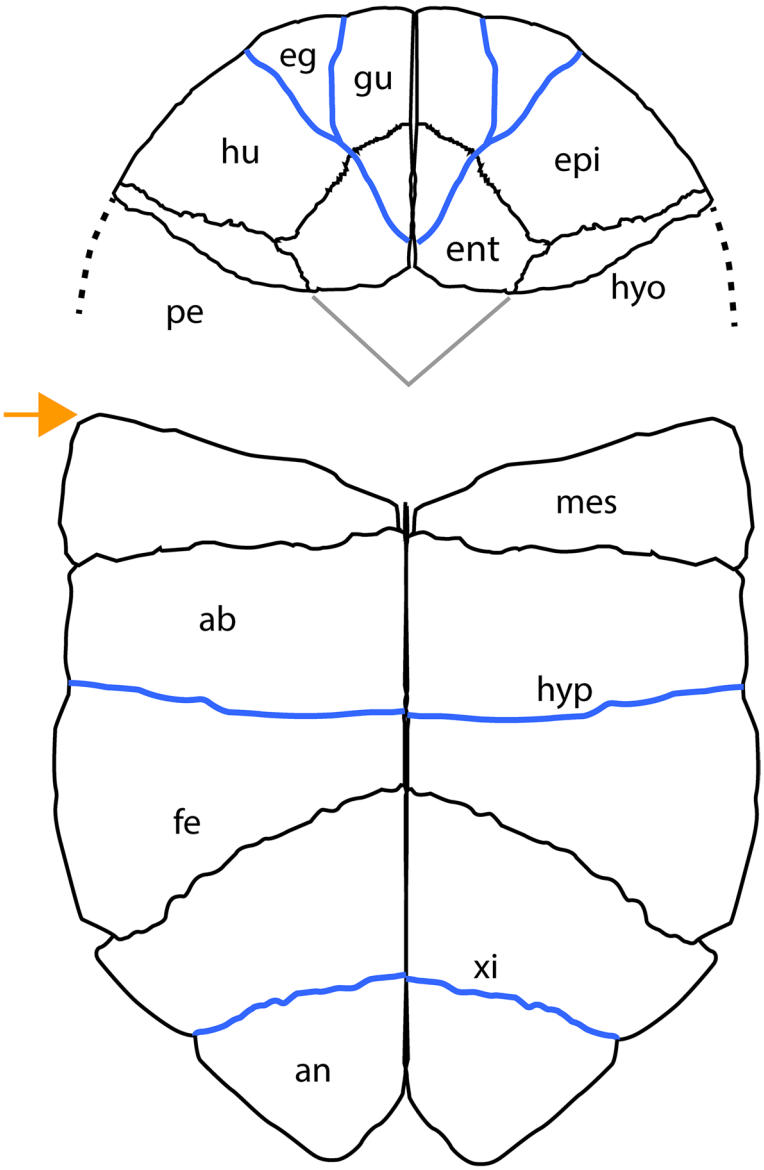

Fig. 9. Plastral reconstruction of *Pelusios awashi* sp. nov. Abbreviations: ab = abdominal scale, an = anal scale, ent = entoplastron, epi = epiplastron, eg = extragular scale, gu = gular scale, hu = humeral scale, hyo = hyoplastron, hyp = hypoplastron, mes = mesoplastron, pe = pectoral scale, xi = xiphiplastron. Blue lines indicate sulci and orange arrow indicates location of plastral hinge. Dotted black lines indicate estimated shape of lateral hyoplastral margin. Reconstruction utilizes two unassociated specimens: A.L. 2137-1a for the anterior plastral lobe and A.L. 161 – 26 for plastron posterior to hinge, so the components may not be to the same scale. Orange arrow indicates location of plastral hinge.

The basisphenoid is generally flat and approximately triangular in shape with curved edges that are concave laterally (Fig. 3B). It is located in the center of the basicranium and forms the floor of the cavum cranii. Both the basisphenoid and the prootic contribute to the foramen posterius canalis carotici interni, though the extent of the ventral exposure of the prootic is uncertain due to localized damage.

Carapace. A.L. 380-3 includes a partial articulated carapace that is missing its anterior end, as well as most of the peripherals except at the posterior margin (Fig. 4). The specimen preserves a seemingly natural shape that is clearly domed and held in articulation by a mass of medium sandstone that fills much of the dorsal concavity of the carapace (Fig. 4C-D). Sutures are well defined on the surface of the carapace and visible without magnification, but they are very fine. In contrast, sulci are shallow and relatively wide (~ 3 millimeters [mm]) with raised edges formed by the surrounding bone. The recessed areas are generally flat, though they are frequently marked by additional longitudinal marks and small pits. The carapace does not have any particular pattern of ornamentation, but its surface is uneven and somewhat undulating, with a midline elevation at the level of approximately the sixth neural (Fig. 4C-D). The nuchal is missing along with the most anterior neurals (Fig. 4A-B). Five neurals are preserved, and the posterior four are complete (Fig. 4A-B). The anteriormost neural

A.L. specimen	Submember	Elements	Figure
251 – 39	SHT	Bilateral hypoplastra including right inguinal buttress	7 A-D
380-3	SH-4	Articulated partial carapace including costals, posterior peripherals, neurals, pygal and suprapygal	4
161 – 26	DD-2	Right meso-, hypo-, and xiphiplastron	7I-P
366-4	DD-2	Partial right plastron including meso-, hypo-, xiphi-, epi- and entoplastron	6 A-D, 7E-H
207 – 15	DD-2	Partial cranium	2, 3
333w-510	DD-2	Right xiphiplastron	5 A-D
333w-511	DD-2	cf. juvenile right xiphiplastron	5E-H
333w-512	DD-2	Costal fragment with crocodile bite marks	5I-L
333w-513	DD-2	cf. juvenile right epiplastron	5 M-N
333w-514	DD-2	Right peripheral 11	5O-V
2137-1a	Unknown	Complete right epiplastron, partial left epiplastron, partial right hyoplastron and partial entoplastron	6E-H
2137-1b	Unknown	Pygal	6 M-P
2138-1a	Unknown	Right costal 8	6I-L
2138-1b	Unknown	Left xiphiplastron	6Q-T

Table 1. Specimens of *Pelusios awashi* sp. nov. included in the current study.

is incomplete and its posterior end is approximately rectangular. The next neural is interpreted as the fifth in the series and is roughly hexagonal in shape with rounded corners. The sixth neural is also hexagonal and similar in width to the fifth, but shorter. The seventh neural is similar in proportion to its predecessor, but its lateral edges are more evenly divided between its anterior and posterior faces (Fig. 4B). The last (eighth) neural in the series is distinctly hexagonal and coffin-shaped, tapering posteriorly to form a point contact with the suprapygal (Fig. 4B). The preserved costals of A.L. 380-3 have relatively consistent lengths between their medial and lateral ends and are curved posteriorly. The two most posterior costals differ in the tapering of their medial sides. Costals 6, 7, and 8 are preserved on both sides of A.L. 380-3, and the right side also includes costals 4 and 5 (Fig. 4B). Each costal contacts the posterior face of the lateral side of its corresponding neural as well as the anterior face of the next posterior neural in the series. The right fourth costal differs from this pattern by contacting the fourth and fifth neurals near their junction, but damage and surficial matrix somewhat obscure this area. The eighth costal also differs from other costals by contacting only one neural, and it also contacts the suprapygal posteriorly (Fig. 4A-B).

An isolated medial fragment of a costal (A.L. 333w-512) demonstrates contact between vertebral and pleural scales on its dorsal surface (Fig. 5I-L). The order of the costal may not be unequivocally determinable out of articulation, but interpleural sulci only cross even-numbered costals in *Pelusios*[27]. Considering the horizontal direction of the intervertebral sulcus, the costal is likely the fifth on the left side. A prominent but low, medially oriented ridge on the ventral surface of A.L. 333w-512 represents a rib head, and the specimen has a taphonomic pit on both the dorsal and ventral surfaces. These resemble tooth marks from a predator and are described and discussed below (Fig. 5I-L). The isolated right eighth costal A.L. 2138-1a preserves contact between the fourth pleural and fifth vertebral scales across most of its width as well as the corner of the fourth vertebral scale, which overlaps slightly onto its medial tip (Fig. 6I-L). There are two short, similarly sized ribs heads on the ventral surface of the medial end of the costal that are likely associated with sacral ribs, which are sometimes attached or fused to posterior costals in fossil turtles[51] (Fig. 6K-L).

Peripherals are only present along the posterior margin of A.L. 380-3 and include peripherals 9 through 11 on the left side, peripheral 11 on the right side, and an attached portion of peripheral 10 (Fig. 4B). Each peripheral has a similar proportion of nearly equal length and width, and they are moderately scalloped along their free edges. Peripherals are also curved in cross section and upturned toward the shell margin in A.L. 380-3 and 333w-514 (Figs. 4C-D and 5O-V). The suprapygal of A.L. 380-3 is approximately triangular, with curved lateral edges that are convex laterally and a posterior border that is similar but posteriorly concave in its contact with the pygal (Fig. 4B). The suprapygal also contacts the eighth neural, and bilateral posteriormost costals and peripherals. The pygal of A.L. 380-3 is roughly trapezoidal with a similar length to width, and it is slightly narrower anteriorly. It has convex, curved edges, except posteriorly, where it is slightly indented at the midline (Fig. 4B). Similar morphology characterizes the isolated pygal A.L. 2137-1b (Fig. 6M-P). As mentioned above, sulci marking the borders between the carapacial scales of A.L. 380-3 are wide and clearly marked except in areas with surface abrasion or encrusted matrix (i.e., near the anterior midline) (Fig. 4). Sulci traverse the posterior halves of the dorsal surfaces of the fourth, sixth, and eighth costals, marking the boundaries between the second, third, and fourth pleural scales, the fourth and fifth vertebral scales, and the pleural-costal border. This final boundary occurs on the dorsal peripheral surfaces, and the last (eleventh) peripherals are overlapped by four scales— the fourth peripheral, fifth vertebral, and marginals 11 and 12 (Fig. 4B). The third vertebral scale of A.L. 380-3 is obscured laterally on the right side by damage and matrix. The fourth vertebral scale is longer than wide and the fifth vertebral has the opposite proportions of the fourth. The junction of peripheral, vertebral, and marginal scales is also visible on the dorsal surface of the isolated eleventh peripheral 333w-514 (Fig. 5O-V).

Plastron. The plastron of *Pelusios awashi* sp. nov. is best represented by the area posterior to the plastral hinge at the hyoplastron-mesoplastron junction along the base of the anterior plastral lobe. The anterior plastral

lobe is the mobile portion of the plastron and is known for *Pelusios awashi* sp. nov. from two specimens— A.L. 366-4 and A.L. 2137-1a (Fig. 6A-H). Both include epiplastra and portions of adjacent elements are articulated in the latter (Fig. 6E-H). An additional, isolated left epiplastron A.L. 333w-513 is probably from a juvenile and was recovered from A.L. 333, the "First Family" locality (Fig. 5M-N). Based on these specimens, the epiplastron of *Pelusios awashi* sp. nov. can be characterized as thicker toward the anterolateral free margins. It has a robust midline contact with its contralateral counterpart, and an irregular, jagged suture shared with the hyoplastron that is convex posteriorly (Figs. 5M-N and 6A-H). The ventral epiplastral surfaces of A.L. 2137-1a and A.L. 333w-513 are marked by sulci from both gular and extragular scales (Figs. 5M-N and 6E-H). This area on A.L. 366-4 is poorly preserved and concealed by finely encrusted matrix (Fig. 6A-D). Where visible, the extragular scales are triangular and almost reach the entoplastron-epiplastron suture posteriorly, but do not overlap onto the entoplastron (Figs. 5M-N and 6A-D). However, the gular scale overlaps onto the entoplastron and reaches approximately the center of the entoplastron (Figs. 5M-N and 6E-H).

The entoplastron of *Pelusios awashi* sp. nov. is roughly diamond shaped and slightly longer than wide (Fig. 6A-H). In A.L. 366-4, the entoplastron has a prominent, ventrally-projecting point at its anterior tip, a slight posterior ridge along the midline, and an uneven posterior edge (Fig. 6A-D). Entoplastra marked by a gular-humeral sulcus on their anterior ventral surfaces, though these indications are mostly covered by thin matrix in the juvenile (Fig. 6C-D). The hyoplastron of *Pelusios awashi* sp. nov. is only preserved in A.L. 2137-1a, and only by its irregular anterior junction with the ento- and epiplastron (Fig. 6A-H). The ventral surface of A.L. 2137-1a is curved slightly dorsally to the lateral edges, and the bone thickness is lesser than that of the posterior plastron. Unfortunately, the current samples do not preserve the posterior margin of the hyoplastron, so its contribution to the plastral hinge formed with the mesoplastron cannot be assessed in detail. Carapacial tooth traces. As mentioned above, the likely fifth left costal A.L. 333w-512 has a taphonomic mark on both the dorsal and ventral sides (Figs. 5O-V and 7). The dorsal mark is ovoid, measuring 7.07 mm across its longest dimension and 4.36 mm in its orthogonal diameter (Fig. 8A). The crack within the ventral pit resembles those caused by the prominent carina of crocodile teeth, which can create a subscore that bisects the larger mark. A smaller, ovoid subscore is also present in the dorsal pit, likely indicating deeper penetration beyond the cortical surface. The ventral mark is more subcircular and contains an obliquely oriented crack (Fig. 8B). The diameter of the pit along the axis of the crack is 5.55 mm, and the orthogonal pit diameter is 4.65 mm. Both marks crushed the superficial cortical surface and left bowl-shaped depressions without evidence of lateral movement and potentially reflect the tooth crown shape of the trace maker. The diameters of each mark are similar to the tip diameter of large crocodilian teeth found at Hadar (Fig. 8C).

Several specimens demonstrate the morphology of the more posterior elements of the plastron (Fig. 7E-P). The mesoplastron of *Pelusios awashi* sp. nov. is a thick, wedge-shaped plate of bone that has a very short midline contact with its contralateral side and is robustly articulated along a nearly transverse suture it shares with the hypoplastron. The mesoplastron is continuous in thickness and orientation with the hypoplastron, and its antero-lateral corner curves slightly dorsally. The anterior edges of the mesoplastra form the plastral hinge in modern *Pelusios* spp., which is often perpendicular to the midline (~ 180° across the anterior edge of the mesoplastra). However, these edges are directed posteromedially toward the midline in *Pelusios awashi* sp. nov., and the angle between them is approximately 145°. The posterior suture of the mesoplastron is sturdy and similar to other plastral sutures posterior to the hinge. However, the anterior margin of the mesoplastron is quite different. Its surface is smoother than that of sutures, and lacks jagged, tooth-like structures. Instead, there are rows of low, parallel oblique striations along the anterior edge, along with rows of fine foramina. Another, larger row of low perpendicular ridges follows the edge on the ventral side of the mesoplastron. There are also thin terraces of bone that run parallel to the suture on the ventral surface, which are interpreted as the edges of the abdominal-pectoral sulcus which likely coincided with the suture, as in modern *Pelusios*[30].

The hypoplastra are the largest bones of the plastron in *Pelusios awashi* sp. nov. They are located between the mesoplastra anteriorly and the xiphiplastra posteriorly, and there is no evidence of a central fontanelle (Fig. 7). The suture between the mesoplastron and hypoplastron on each side is nearly horizontal though angled slightly posterolaterally. The suture between the hypoplastron and xiphiplastron is also directed posterolaterally, but at an angle of approximately 121° from the midline. This suture is irregular and jagged, and a posteriorly directed, toothed articular projection occurs along its lateral half, just medial to the rim of thicker bone that comprises the posterior plastral margin (Fig. 7A-L). The lateral edge of the hypoplastron is curved, especially posterior to the inguinal buttresses, and the flat dorsal surface of this edge expands posteriorly (Fig. 7A-B, E-F, I-J). This area is lateral to a longitudinal ridge marking the skin contact with the hypoplastron, and the abdominal-femoral sulcus continues onto this area from the ventral side of the bone (e.g., Fig. 7A-B). The abdominal-femoral sulcus is gently curved and convex posteriorly, crossing the ventral surface of the hypoplastron (Fig. 7C-D, G-H, K-L). The inguinal buttresses are oriented posterodorsally and project prominently from the dorsal side of the hypoplastra near their anterolateral corners (Fig. 7A-B, E-F, I-J, M-P). The xiphiplastra of *Pelusios awashi* sp. nov. are the most posterior bones of the plastron and form a wedge anteriorly that fills the space along the midline between the hypoplastra (Fig. 7E-L). The xiphiplastra are continuous in thickness and orientation with the hypoplastral plates, and curve slightly dorsally at their posterior ends (Fig. 7M-P). The xiphiplastra have a lateral edge that continues the posteromedial curvature of the hypoplastra posteriorly. The femoral-anal sulcus is straight and crosses the ventral surface of the xiphiplastra at an angle that is similar to that of the hypo-xiphiplastral suture (Figs. 6Q-T and 7G-H and K-L). One specimen (A.L. 333w-510), there is an additional superficial mark traveling from approximately the medial side of the femoral-anal sulcus, where it nearly disappears medially, to the posteriormost point of the xiphiplastron (Fig. 5C-D). This is interpreted as a potential trace that was emplaced postmortem by some scavenger organism. The relatively thick lateral margin of the xiphiplastron is indented slightly at the femoral-anal sulcus and continues to a point at the posteriormost end of

the xiphiplastron. The xiphiplastra maintain their thickness, which is greatest along the lateral margin, almost to the posterior end of the bone. The posterior ends of the xiphiplastra leave a medial space between them that forms a distinct anal notch with an inverted V-shape (Fig. 7E-H). As a classic and unambiguous synapomorphy in pleurodiran turtles, the pelvic girdle is sutured to the plastron[17,52]. This articulation in *Pelusios awashi* sp. nov. occurs as two scars on the ventral side of each xiphiplastron. The pubic scar is more anterior and lateral with an approximately ovoid to subtriangular shape that is slightly longer than wide (Figs. 5A-H, 6Q-R and 7I-J). The ischial scar is also approximately ovoid, and more antero-posteriorly flattened in the juvenile specimen A.L. 2138-b (Fig. 6Q-R). It is adjacent to the midline as well as the thickest portion of the posterior end of the dorsal xiphiplastron. The femoral-anal sulcus courses between the pelvic articulations on the opposite (ventral) side of the xiphiplastron (Fig. 5A-D).

Discussion

Comparison of *Pelusios awashi* sp. nov. With other *Pelusios* species

Pelusios awashi sp. nov. is larger than most modern *Pelusios* species, which have a straight carapace length of less than 30 cm, but falls within the size range known for the genus[26] (see Supplementary Table S1). The most complete shell specimen (A.L. 380-3) of the new species was estimated to be 42 cm long based on proportional comparisons with modern *P. sinuatus*[25,53–55]. This estimate is greater than all other modern congenerics except *P. sinuatus*, and none of the next smaller species that are equal to or larger than 30 cm (*P. chapini*, *P. niger*, *P. bechuanicus*, and *P. gabonensis*) are known from areas outside of eastern Africa[53,56–60].

The interorbital region is also relatively wide in the new species. The ratio of interorbital distance to length of the supraocular cranial scale at the midline in *Pelusios awashi* sp. nov. is greater than that of *P. nanus*, *P. bechuanicus bechuanicus*, *P. bechuanicus upembae*, *P. rhodensianus*, *P. castaneus castaneus*, and *P. sinuatus*[27]. This value (148%) exceeds the greatest values of these species and only falls into the relatively broad range measured for *P. subniger*, though it substantially exceeds the mean of the latter[27]. Behind the new species, the next greatest mean belongs to the "blunt-headed" *P. bechuanicus bechuanicus* (113%), and the "relatively long-snouted" *P. sinuatus* has the smallest mean (~ 67%)[27]. Additionally, the ratio of the distance between lateral orbital ends to anterior-posterior length of the entire skull (measured as ventral length from the tip of the premaxilla to the occipital condyle) is 0.70 in *Pelusios awashi* sp. nov., compared to 1.05 in *P. sinuatus*[61], 1.12 in *P. castaneus*[17], and 1.23 in *P. niger*[50].

Pelusios awashi sp. nov. is consistent with many extant *Pelusios* species (e.g., *P. subniger*, *P. bechuanicus bechuanicus*, *P. rhodesianus*, *P. castaneus* except *P. castaneus castanoides*), which have a typical arrangement of eight neurals in a continuous series[27]. In contrast, most *Pelusios sinuatus* and *P. castaneus castanoides* have six or seven neurals without an eighth neural and may have a reduced or absent seventh neural[27]. *Pelusios awashi* sp. nov. represents an uncommon neural variation by contact between the eighth neural and the suprapyal, a condition which is only otherwise reported in some individuals of *P. rhodesianus*[27]. Multiple specimens of *Pelusios awashi* sp. nov. demonstrate moderately convex lateral hypoplastral margins, unlike the more curved convexities of *P. subniger* and *P. castaneus castanoides*, and the straighter margins of *P. rhodesianus* and *P. sinuatus*[27],

A comprehensive comparison of *Pelusios awashi* sp. nov. with all modern *Pelusios* species is infeasible due to incomplete osteological data for some taxa (see Supplementary Table 1). Many species are also classified based on non-osteological traits, such as coloration, scalation, or genetic profiles[8,11,27]. However, modern *Pelusios* spp. have been historically divided into two groups based on plastral morphology: the *adansonii-gabonensis* group with a short bridge and medially tapered mesoplastra, and the *subniger* group with a longer bridge and non-tapered mesoplastra[8,18]. Within this framework, the mesoplastra of *Pelusios awashi* sp. nov. are acutely tapered medially as in species of the *adansonii-gabonensis* group (e.g., *Pelusios gabonensis*), in contrast with the straighter plastral hinges of *Pelusios sinuatus* and *Pelusios subniger*[27,30,52,53]. The ratio of the width of the abdominal-femoral sulcus to the width of the pectoral-abdominal sulcus further distinguishes *Pelusios awashi* sp. nov. from congenerics, with values of 1.13 and 1.06 for specimens A.L. 366-4 and A.L. 161-26, respectively (average: 1.095), exceeding the means of *P. sinuatus*, *P. nanus*, *P. subniger*, *P. bechuanicus bechuanicus*, *P. bechuanicus upembae*, *P. rhodesianus*, and *P. castaneus*[27]. Some Hadar Fm. fossils were previously reported as resembling *Pelusios gabonensis* as part of an informal comparison between extinct and extant species, and particularly large specimens were documented from the Denen Dora Member[16]. *Pelusios awashi* sp. nov. differs from the holotype of *Pelusios gabonensis* by its larger adult size, a fifth vertebral scale that is mediolaterally wider than the fourth and scalloping on its posterior peripherals and pygal, though the holotype of *P. gabonensis* is a juvenile and carapacial scales can vary intraspecifically[62,63]. Table S1 summarizes the carapace length and plastral hinge shape of modern *Pelusios* species.

A comparison of *Pelusios awashi sp*. nov. with *Pelusios rusingae* shows similarities in plastral proportions consistent with the *adansonii-gabonensis* group for both species, but the latter had nearly half (~ 58%) the carapace length of the new species[18]. Medial tapering of the mesoplastra in the new species is similar to that described for the oldest species of the genus (i.e., Early Miocene *P. rusingae*), demonstrating a plesiomorphic stage in the evolutionary expansion of the mesoplastron, a critical component of the plastral hinge[18]. The neural series of *Pelusios rudolphi*, along with its two topotypes from Omo and *Pelusios sinuatus* (with which it is synonymized), is reduced to five or six elements. This contrasts with *Pelusios awashi* sp. nov., which has a complete neural series with eight elements extending to the suprapygal[25,27]. Furthermore, *Pelusios rudolphi* can be distinguished from the new species by its fourth vertebral scale, which is proportionally narrower and more rectangular than hexagonal in shape[21]. Fossil specimens of *Pelusios sinuatus* from Oldupai Gorge are distinct from *Pelusios awashi* sp. nov. by having a straighter plastral hinge[21,64]. Additional *Pelusios sinuatus* fossils from Chad and Lake Turkana also lack medial mesoplastral tapering[27,64].

Evolution of plastral kinesis within *Pelusios*

A plastral hinge is unique to *Pelusios* among pleurodires[8,17,27,29]. Plastral kinesis has evolved multiple times in turtles involving a variety of non-homologous structures, including anterior and posterior hinges in *Kinosternon*, and only anterior hinges in *Cuora*, *Planetochelys*, *Cardichelyon rogerwoodi*, and *Ptychogaster*[29,65–70]. Such mechanisms arose from minor modifications to syndesmotic joints, and all plastral sutures have the potential to become kinetic[70]. Among modern turtles with closeable shells, only the North American box turtle *Terrapene* is not fully aquatic[65].

In *Pelusios*, kinesis occurs between the hyo- and mesoplastra, separating the pectoral and abdominal scales, and typically allows nearly complete anterior shell closure[29,51]. Some sources have incorrectly placed the hinge elsewhere[8,70,71]. While biomechanical studies of plastral kinesis have primarily focused on cryptodiran emydids[51,65,67,72,73], the anatomy and mechanics of hinge closure in *Pelusios* have been described in detail[29]. The preserved plastral hinge of *Pelusios awashi* sp. nov. thus provides insight into the evolution of the structure within the genus (Fig. 8). Medial tapering is within the mesoplastral variation seen in panpleurodires, and *Pelusios broadleyi* is the only species within the genus to have an immobile plastron, possibly due to a central plastral fontanelle[28,71,74]. A straight hinge (180°) that maximizes mobility is typical in *Pelusios bechuanicus bechuanicus*, *P. carinatus*, *P. cupulatta*, *P. niger*, *P. sinuatus*, and *P. subniger*[8,9,25,27,62]. In contrast, *Pelusios gabonensis* has a 145° hinge[62], closely resembling that of *Pelusios awashi* sp. nov., and *Pelusios rusingae* also exhibited medial tapering[18,27] (Fig. 9).

Body size variation within Pelusios

The large body size of *Pelusios awashi* sp. nov. and *Pelusios sinuatus* may be related to shared environmental factors. *Pelusios sinuatus* is widespread in eastern Africa, ranging from Ethiopia and Somalia south to South Africa and Eswatini, and fossil evidence indicates an even broader historical range[12,54]. The species currently reaches its largest size in the northern part of its range near the equator, with reported maximum shell lengths reaching 55 cm[53,75], and there is significant size variation between wild and museum specimens from different regions[53]. Habitat influences African terrapins in a similar way to the aquatic painted turtle *Chrysemys picta*, where maximum body size is achieved by more carnivorous populations inhabiting rivers, and smaller herbivorous turtles living in marshes[27,76]. For instance, northern populations of *Pelomedusa subrufa* inhabit seasonal swamps and temporary pans and reach a maximum carapace length of approximately 20 cm, while in southern populations that are free of competition from *Pelusios*, *Pelomedusa subrufa* that occupy rivers and other permanent water sources can attain 32.5 cm[77,78]. Similarly, though *Pelusios sinuatus* can exceed 50 cm, shell lengths of 30 cm are common in rivers and large lakes, whereas turtles inhabiting small rivers and areas with dams are typically smaller and may not surpass 20 cm[27]. The relatively large size of *P. awashi* sp. nov. suggests that it may have inhabited relatively large bodies of water, which were present in submember DD-2 as a system of fluvial or fluvial-deltaic channels perhaps 40 m (m) across and 3 m deep[33].

Paleoecological inferences for *Pelusios Awashi* sp. nov

The maxilla of *Pelusios awashi* sp. nov. is notably broad and includes an expansive triturating surface that is typically associated with a durophagous diet in many turtle groups[78]. Extant *Pelusios* species such as *P. sinuatus* and *P. castaneus* feed extensively on large (~ 50 mm) pulmonate (air-breathing) snails in lakes of Malawi[27,79]. Similarly, other *Pelusios* species (i.e., *P. niger*, *P. adansonii*, *P. nanus*) consume varying proportions of hard-shelled prey such as gastropods, crustaceans, and bivalves, and durophagous behavior was shown to increase with turtle body size[80]. Mollusks are known from numerous lacustrine strata of the Hadar Fm., and the maxillary morphology and large body size of *Pelusios awashi* sp. nov. suggest that these prey may have been an important dietary component for the turtles[81].

Despite morphological differences, *Pelusios awashi* sp. nov. and *Pelusios sinuatus* are similarly large in body size and probably had comparable modes of locomotion (i.e., bottom walking), suggesting possible phylogenetic and climatic niche conservatism[82]. In turtles, these factors can lead to the retention of ancestral climate preferences, allowing species to persist in similar environments and occupy analogous niches despite environmental changes over time[49,83,84]. The mid-Pliocene climate at Hadar was significantly wetter than today, but each could be characterized as having strong monsoonal seasonality and savanna or grassy woodland ecosystems[85]. Savannas are characterized by the coexistence of grasses and trees and comprise nearly half the surface of sub-Saharan Africa[27,34,95]. Pollen data from the DD-2 submember indicate dry grassland with mean annual precipitation (MAP) estimated at 900 mm (modern MAP = ~ 500 mm), which was split between two rainy seasons that could fluctuate from 300 to 800 mm per year[85,86]. Isotopic data from mollusks and paleosols of the Hadar Fm. suggest a strong summer monsoon and a dry season lasting only three months– a seasonal regime unlike any in present-day East Africa[81]. Paleosols dominated by Vertisols and smectite-rich mudstones further indicate seasonal moisture variation in a semi-arid to sub-humid climate[87,88]. Fluctuating lacustrine conditions were prominent in Hadar, particularly from the upper Sidi Hakoma to Denen Dora Members (SH-4 through DD-2 submembers)[33]. Wetlands with grasses and MAP estimates of 800–900 mm are indicated for SH-4[85]. Diatoms and ostracods suggest variable lake salinity, typically oligohaline to mesohaline, consistent with tolerances of modern *Pelusios* species, which are not known from highly saline lakes[33,89,90]. Extinct *Pelusios sinuatus* populations may have survived in freshwater inlets of mudflats, even during low lake levels[22]. The Denen Dora Member (3.26–3.2 Ma) also records fluvial environments, including distributary channels and delta plains, with seasonal flooding[31,33].

Pelusios species are typically adapted to specific river basins and occur in a variety of modern habitats, including wet and dry savanna environments[27]. *Pelusios sinuatus* favors relatively deep perennial lakes and rivers, utilizing logs and sometimes hippos for basking, and migrates to seasonal water bodies during rains[25]. Nesting can occur up to 500 m from water, and eggs are vulnerable to predators like mongooses and *Varanus niloticus*[30]. During droughts, *Pelusios sinuatus* (and also *Pelusios castaneus*) may aestivate in riverbank hollows,

and it is sometimes preyed upon by crocodiles[25,27,91]. *Pelusios sinuatus* is known to scavenge crocodile kills, and it also eats fallen bird nestlings, floating fruit, and ticks from buffalo[53]. It has been documented in sympatry with *Pelusios subniger* and *Pelomedusa subrufa* in riverbeds and seasonal pans[25,27]. Other *Pelusios* spp. demonstrate tolerance to a wide variety of habitats, such as *P. nanus*, which inhabits moist savannas and forest-savanna mosaics in the southern portion of the Congo Basin, and *P. carinatus*, which is the ecological equivalent of *P. sinuatus* in the Congo Basin[27]. *Pelusios awashi* sp. nov. may have had similar adaptations to Hadar's dynamic environments, thriving in seasonal wetlands with both permanent and ephemeral water sources.

A carapace fragment from A.L. 333w (A.L. 333w-512) bears superficial pits consistent with crocodile tooth marks[96] (Figs. 4I-L and 7). While bite mark size can aid in identifying trace makers[97,98], it is influenced by bite force and dental morphology, in addition to bone density of the bite recipient[98,99]. The pits on A.L. 333w-512 resemble those from Plio-Pleistocene *Crocodylus* spp. at Oldupai Gorge[96] and match the dimensions of a large *Crocodylus* tooth from Hadar (A.L. 834-1), with a crown diameter of 5.28 mm and height of 40.26 mm. The relatively medial placement of both pits are inconsistent with the "nutcracker technique" observed in modern crocodylian predation, where shells are bitten perpendicularly on the bridge to fracture the bridge and expose interior tissue[100]. The ventral mark likely occurred later, possibly postmortem or is from another individual, since a single bite is unlikely to produce marks on both sides of a medial costal element. This pattern suggests that the marks occurred during disarticulation, perhaps while the tracemaker was scavenging. Bite marks on turtle shells are frequently attributed to crocodyliforms[101–112]. These traces illustrate how prey anatomy influences both feeding behavior and trace expression. Crocodile feeding marks from Oldupai Gorge were incorporated into models of hazards and resources for co-occurring hominins[113,114].

Implications for early hominin paleoecology and resource use

Numerous fossils of *Pelusios awashi* sp. nov., including the holotype A.L. 207 − 15, were recovered from the DD-2 submember, which includes the highly fossiliferous locality A.L. 333 that produced the renowned *Australopithecus afarensis* "First Family" assemblage[92,93] (Table 1). During DD-2 times, A.L. 333 was located on a delta plain transitioning from lacustrine to fluvial environments, with low-energy, non-catastrophic seasonal flooding and distributary channels[89,93,94]. Rhizoliths and lithological evidence suggest scattered riverine vegetation but probably not large trees. Mammalian faunal analyses indicate that the A.L. 333 landscape supported brush and woodland habitats, including wetlands, with hominins occupying seasonally dry, grass-dominated plains[85,92,95]. *Pelusios* fossils from A.L. 333 were found alongside *Clarias* catfish, a crocodilian scute, and *Pelomedusa* fragments. Given the ecology of the similarly distributed *Pelusios sinuatus*, *Pelusios awashi* sp. nov. may have exhibited comparable adaptations to seasonal wetlands, thereby benefiting from the high biotic productivity of the Hadar Fm.[1,95].

There has been no direct evidence of foraging on terrapins by sympatric *Australopithecus afarensis* (i.e., cut marks) at Hadar, but co-occurrence of the two taxa suggests the possibility of overlap in their habitats, especially considering their mutual dependence on aquatic resources and the capacity for terrestrial overland travel demonstrated by modern *Pelusios*[115,116]. It has been proposed that *Paranthropus boisei* may have been responsible for collecting *Pelusios sinuatus* at Oldupai Gorge since the greatest number of these common fragments have been found at local Oldowan hominin sites (Bed I and lower Bed II) that include possible lake margin terrapin habitats[22,117]. However, other hominin species (i.e., *Homo habilis*) may have also been responsible. Oldupai hominins likely also produced substantial accumulations of fish remains dominated by (80–90%) catfish[118]. Large catfish (e.g., *Clarias*) are known from Hadar[1] and could have been foraged without tools, along with mud terrapins[115,116]. Both catfish and terrapins are particularly vulnerable in their natural habitats during their seasonal reproductive cycles and both venture overland in search of appropriate aquatic habitats. They were potentially protein-rich aquatic resources, and since their acquisition was not technologically dependent, may have formed a regular component of opportunistic hominin diets whenever environmental circumstances allowed[119]. The incorporation of diverse animals, and especially those from the lacustrine food chain added critically nutritional components to hominin diets that could have contributed to the evolution of larger brains in later Pliocene hominins (e.g., *Homo*)[116].

Conclusions

Pelusios awashi sp. nov. is described from a holotype skull, the first known from the fossil record of the genus, and shell material from multiple individuals from the Pliocene Hadar Fm. in Ethiopia. The new species is larger than nearly all modern *Pelusios* representatives and has a carapace length within the range of the largest species, *P. sinuatus*. The new species also differs in several important aspects from modern and fossil congenerics in having a proportionally wider skull with a wider interorbital region and shorter face that is relatively broader and more rounded in dorsal view. Though its anterior portion is missing, the carapace differs from other *Pelusios* species by having a complete neural series that reaches the suprapygal. The plastron differs from all modern species except *P. gabonensis* by having mesoplastra that are substantially tapered medially. This deviation from a straight contact between the hyo- and mesoplastra represents the plesiomorphic condition of the genus and is related to a kinetic anterior plastral lobe, a defining trait of *Pelusios* among pelomedusid turtles.

The similarity in size and geographic location between *P. awashi* sp. nov. and both modern and fossil representatives of *P. sinuatus* suggest that these taxa preferred similar habitats, particularly freshwater channels near river mouths and along nearby lake shores. This is likely considering prevalent conservatism in shell morphology among both aquatic and terrestrial turtles that is related to both climate and niche occupation. Paleoenvironments that include these preferred habitats (i.e., lakeshores and adjacent shallow freshwater inputs) have also been reconstructed for fossil hominin sites at Hadar and Oldupai Gorge, and were characterized by strong seasonality, high annual rainfall, and mesic conditions. The presence of both hominin and large mud terrapin fossils at these sites highlights the importance of these habitats for both groups and aligns with known

patterns of hominin utilization of aquatic resources. Crocodile bite marks on fossils of *Pelusios awashi* sp. nov. support prior evidence of crocodile scavenging near A.L. 333. These findings indicate that crocodile predation included chelonivory on the largest known aquatic turtle at Hadar and likely posed risks to coeval hominins in lake-margin habitats.

Materials and methods

Fossils in this study are from the collections of the National Museum of Ethiopia in Addis Ababa. One of us (CJC) is the current director of the Hadar Research Project (HRP), and permission to study this material was also granted by the Ethiopian Heritage Authority. Fossil specimens included in this study (see Fig. 1) were collected in 1975, except for A.L. 251 – 39 that was collected in 1976 and A.L. 207 – 15, collected in 1990. Specimens numbered A.L. 2137 and 2138 did not include submember or geographic provenance data. No specimens representing the shell of *Pelusios awashi* sp. nov. were associated with the holotype skull A.L. 207 – 15 (Table 1). However, it is most parsimonious that all the material described here belongs to the same species, as the localities that produced the fossils were constrained to a small temporal interval and geographic area (Fig. 1), and there was no evidence of another species of *Pelusios* (or other large aquatic turtle) from Hadar deposits housed at the National Museum of Ethiopia. We utilize the anatomical terminology and taxonomic scheme of turtles produced by Joyce[71] unless otherwise noted. Phylogenetically defined clade names follow PhyloCode guidelines[15,120]. Measurements were taken from high resolution digital photographs using ImageJ software[121]. Figures were created with Adobe Creative Cloud software[122].

Data availability

Datasets generated and/or analyzed during the current study are available from the corresponding author on reasonable request.

Received: 10 May 2025; Accepted: 14 October 2025
Published online: 19 November 2025

References

1. Campisano, C. J., Rowan, J. & Reed, K. E. in *African Paleoecology and Human Evolution.* (eds S.C. Reynolds & René Bobe) Ch. 18, 214–228Cambridge University Press, (2022).
2. Wagler, J. G. *Natürliches System Der Amphibien: Mit Vorangehender Classification Der Säugethiere Und Vögel: Ein Beitrag Zur Vergleichenden Zoologie* (JG Cotta, 1830).
3. Wermuth, H. & Mertens, R. *Schildkroten, Krokodile, Bruckenechsen* (G. Fischer, 1961).
4. Wermuth, H., Mertens, R., Testudines & Crocodylia Rhynchocephalia. *Das Tierreich* **100**, 1-174, i-xxvii (1977).
5. Gaffney, E. S. & Meylan, P. A. in *The Phylogeny and Classification of the Tetrapods, Volume 1: Amphibians, Reptiles, Birds* Vol. 35A *Systematics Association Special Volume* (ed M.J. Benton) Ch. 5Clarendon Press, (1988).
6. Ernst, C. H., Altenburg, R. G. M. & Barbour, R. W. *In World Biodiversity Database, CD-ROM series, Windows, Version 1.2* (Biodiversity Center of ETI, 2000).
7. Fritz, U. & Havaš, P. Vol. 57 149–368 (Senckenberg Gesellschaft für Naturforschung, (2007).
8. Fritz, U. et al. Molecular phylogeny of African hinged and helmeted terrapins (Testudines: pelomedusidae: *Pelusios* and *Pelomedusa*). *Zoolog. Scr.* **40**, 115–125 (2011).
9. Fritz, U. et al. Weak divergence among African, Malagasy and seychellois hinged terrapins (*Pelusios castanoides*, *P. subniger*) and evidence for human-mediated Oversea dispersal. *Organisms Divers. Evol.* **13**, 215–224 (2013).
10. Stuckas, H., Gemel, R. & Fritz, U. One extinct turtle species less: *Pelusios seychellensis* is not extinct, it never existed. *PLoS One*. **8**, e57116 (2013).
11. Kindler, C. et al. Comparative phylogeographies of six species of hinged terrapins (*Pelusios* spp.) reveal discordant patterns and unexpected differentiation in the *P. castaneus*/*P. Chapini* complex and *P. rhodesianus*. *Biol. J. Linn. Soc.* **117**, 305–321 (2016).
12. Rhodin, A. G. J. et al. in *Chelonian Research Monographs* Vol. 7 (eds Anders G.J. Rhodin et al.) 292 (2017).
13. Vargas-Ramírez, M. et al. Deep genealogical lineages in the widely distributed African helmeted terrapin: evidence from mitochondrial and nuclear DNA (Testudines: pelomedusidae: *Pelomedusa subrufa*). *Mol. Phylogenet. Evol.* **56**, 428–440 (2010).
14. Petzold, A. et al. A revision of African helmeted terrapins (Testudines: pelomedusidae: *Pelomedusa*), with descriptions of six new species. *Zootaxa* **3795**, 523–548 (2014).
15. Joyce, W. G. et al. A nomenclature for fossil and living turtles using phylogenetically defined clade names. *Swiss J. Palaeontology*. **140**, 1–45. https://doi.org/10.1186/s13358-020-00211-x (2021).
16. Lapparent de Broin, F. African Chelonians from the jurassic to present: phases of development and preliminary catalogue of the fossil record. *Palaeontol. Africanus*. **36**, 43–62 (2000).
17. Gaffney, E. S., Tong, H. & Meylan, P. A. Evolution of the side-necked turtles: the families Bothremydidae, Euraxemydidae, and Araripemydidae. *Bull. Am. Museum Nat. History*. **300**, 1–318 (2006).
18. Williams, E. E. *A New Miocene Species of Pelusios and the Evolution of that Genus* (Museum of Comparative Zoology, 1954).
19. Steinthorsdottir, M. et al. The Miocene: The future of the past. *Paleoceanogr. Paleoclimatol.* **36**, e2020PA004037 (2021).
20. Reinach, A. v. Schildkrötenreste Aus dem ägyptischen Tertiär. *Abh. senckenb. Naturf* Ges., Bd **29**, 1–64, (1903). pl. 61 – 17.
21. Arambourg, C. in *MIssion scientifique de l'Omo (1932–1933), t. 1(Géologie-Anthropologie* Vol. 3 461–466, Fig. 479–480, pl. 434–435, 462 tabl. (Muséum national d'Histoire naturelle, (1947).
22. Auffenberg, W. The fossil turtles of Olduvai Gorge, Tanzania, Africa. *Copeia* **1981**, 509–522 (1981).
23. Musiba, C., Gidna, A. & Alene, M. The dawn of humanity: what can paleoanthropologists and geoscientists learn from one another? *Elements* **19**, 75–81 (2023).
24. Guedes, P. et al. Phylogenetic relationships of the West African mud turtle (*Pelusios castaneus*) on the Islands of São Tomé and Príncipe, West central Africa. *Amphibia-Reptilia* **1**, 1–7 (2023).
25. Broadley, D. & Boycott, R. *Pelusios sinuatus* (Smith 1838) – serrated hinged terrapin. *Conserv. Biology Freshw. Turtles Tortoises Chelonian Res. Monogr.* **5**, 036031–036035 (2009).
26. Vitt, L. J. & Caldwell, J. P. *Herpetology: an Introductory Biology of Amphibians and Reptiles* (Academic, 2013).
27. Broadley, D. G. *A Review of the Genus Pelusios Wagler in Southern Africa (Pleurodira, Pelomedusidae)* (National Museums and Monuments, 1981).
28. Bour, R. Note Sur *Pelusios adansonii* (Schweigger, 1812) et Sur Une Nouvelle espèce affine du Kenya (Chelonii, Pelomedusidae). *Studia Geologica Salmanticensia Extra*. **2**, 23–54 (1988).

29. Bramble, D. M. & Hutchison, J. H. A Reevaluation of plastral kinesis in African turtles of the genus *Pelusios*. *Herpetologica* **37**, 205–212 (1981).
30. Boycott, R. & Bourquin, O. *The Southern African Tortoise Book - A Guide To Southern African Tortoises, terrapins, and Turtles* (O. Bourquin, 2000).
31. Taieb, M., Johanson, D., Coppens, Y. & Aronson, J. Geological and palaeontological background of Hadar hominid site. *Afar Ethiopia Nature*. **260**, 289–293 (1976).
32. Tiercelin, J. The pliocene Hadar Formation, Afar depression of Ethiopia. *Geol. Soc. Lond. Special Publications*. **25**, 221–240 (1986).
33. Campisano, C. J. & Feibel, C. S. Depositional environments and stratigraphic summary of the pliocene Hadar formation at Hadar, Afar Depression, Ethiopia. *Geol. Soc. Am. Special Paper*. **446** (08), 179–201. https://doi.org/10.1130/2008.2446 (2008).
34. Owen-Smith, N. *Only in Africa: the Ecology of Human Evolution* (Cambridge University Press, 2021).
35. Wynn, J. G. et al. Stratigraphy, depositional environments, and basin structure of the Hadar and Busidima formations at Dikika, Ethiopia. *Geol. Soc. Am. Spec. Pap.* **446**, 87–118 (2008).
36. Bobe, R., Coelho, J. O., Carvalho, S. & Leakey, M. G. in *African Paleoecology and Human volution.* (eds S.C. Reynolds & René Bobe) Ch. 26, 311–331Cambridge University Press, (2022).
37. Johanson, D. C., Taieb, M., Gray, B. T. & Coppens, Y. Geological framework of the pliocene Hadar formation (Afar, Ethiopia) with notes on paleontology including hominids. *Geol. Soc. Lond. Special Publications*. **6**, 549–564 (1978).
38. Johanson, D. C., Taieb, M. & Coppens, Y. Pliocene hominids from the Hadar Formation, Ethiopia (1973–1977): stratigraphic, chronologic, and paleoenvironmental contexts, with notes on hominid morphology and systematics. *Am. J. Phys. Anthropol.* **57**, 373–402 (1982).
39. Johanson, D. C. et al. Morphology of the pliocene partial hominid skeleton (AL 288-1) from the Hadar formation, Ethiopia. *Am. J. Phys. Anthropol.* **57**, 403–451 (1982).
40. Johanson, D. C., White, T. D. & Coppens, Y. Dental remains from the Hadar Formation, ethiopia: 1974–1977 collections. *Am. J. Phys. Anthropol.* **57**, 545–603 (1982).
41. Kimbel, W. H., White, T. D. & Johanson, D. C. Cranial morphology of *Australopithecus afarensis*: a comparative study based on a composite reconstruction of the adult skull. *Am. J. Phys. Anthropol.* **64**, 337–388 (1984).
42. Kimbel, W. H., Johanson, D. C. & Rak, Y. The first skull and other new discoveries of *Australopithecus afarensis* at Hadar, Ethiopia. *Nature* **368**, 449–451 (1994).
43. Kimbel, W. H. & Delezene, L. K. Lucy redux: a review of research on australopithecus afarensis. *Am. J. Phys. Anthropol.* **140**, 2–48 (2009).
44. Cope, E. D. Sketch of the primary groups of batrachia salienta. *Nat. History Rev. New. Ser.* **5**, 97–120 (1865).
45. Broin, F. d. Les tortues et Le Gondwana. Examen des rapports entre Le fractionnement du Gondwana et La dispersion géographique des tortues pleurodires à partir du Crétacé. *Stvdia Geologica Salamanticensia: Stvdia Palaeocheloniologica*. **2**, 103–142 (1988).
46. Cope, E. D. An examination of the Reptilia and Batrachia obtained by the Orton Expedition to Equador and the Upper Amazon, with notes on other species. *Proc. Acad. Nat. Sci. Philadelphia* **20**, 96–140 (1868).
47. Pérez-García, A. A lower pliocene erymnochelyini turtle (Pleurodira, Podocnemididae) from the Democratic Republic of congo. *Anat. Rec.* **306**, 1396–1410. https://doi.org/10.1002/ar.25073 (2023).
48. Wood, R. *Kenyemys williamsi, a Fossil Pelomedusid Turtle from the Pliocene of Kenya. Advances in Herpetology and Evolutionary Biology* 74–85 (Museum of Comparative Zoology, 1983).
49. Gaffney, E. S. The comparative osteology of the triassic turtle *Proganochelys*. *Bull. Am. Museum Nat. History*. **194**, 1–263 (1990).
50. Gaffney, E. S. Comparative cranial morphology of recent and fossil turtles. *Bull. Am. Museum Nat. History*. **164**, 1–376 (1979).
51. Cordero, G. A. Turtle shell kinesis underscores constraints and opportunities in the evolution of the vertebrate musculoskeletal system. *Integr. Organismal Biology*. **5**, obad033 (2023).
52. Gaffney, E. S., Meylan, P. A., Wood, R. C., Simons, E. & Campos, D. d. A. Evolution of the side-necked turtles: the family Podocnemididae. *Bull. Am. Museum Nat. History*. **350**, 1–238. https://doi.org/10.1206/350.1 (2011).
53. Spawls, S., Howell, K., Drewes, R. & Ashe, J. *A Field Guide To the Reptiles of East Africa: Kenya, Tanzania, Uganda, Rwanda and Burundi* (Academic, 2002).
54. Vamberger, M., Hofmeyr, M. D., Cook, C. A., Netherlands, E. C. & Fritz, U. Phylogeography of the East African serrated hinged terrapin *Pelusios sinuatus* (Smith, 1838) and resurrection of *Sternothaerus bottegi* Boulenger, 1895 as a subspecies of *P. sinuatus*. *Amphibian Reptile Conserv.* **13**, 42–56 (2019).
55. Grant, S. 000116457 *Pelusios sinuatus* Structured Light Mesh [FMNH_12699.ply]. (2020). https://doi.org/10.17602/M2/M116457.
56. Laurent, R. F. & Laurent, R. *A Contribution To the Knowledge of the Genus Pelusios (Wagler)* (Musée Royal de l'Afrique Centrale, 1965).
57. Luiselli, L., Bour, R., Petrozzi, F., Akani, G. & Segniagbeto, G. *105.101-105.108* Vol. 5 (Chelonian Research Foundation and Turtle Conservancy Arlington, VT, 2018).
58. Hewitt, J. Further descriptions of reptiles and batrachians from South Africa. *Records Albany Museum*. **3**, 371–415 (1927).
59. Duméril, A. M. C. & Bibron, G. *Erpétologie générale ou histoire naturelle complète des reptiles*. Vol. 2 680 (Librairie encyclopédique de Roret, 1835).
60. Bour, R. *Pelusios adansonii* (Schweigger 1812) - Adanson's Mud Turtle. Conservation biology of freshwater turtles and tortoises: A compilation project of the IUCN/SSC tortoise and freshwater turtle specialist group. *Chelonian Res. Monographs* **5**, (2008). 017.011–017.014.
61. Hermanson, G. Media 000398470: *Pelusios sinuatus* Cranium [Pelusios_sinuatus_USNM42144.ply]. https://www.morphosource.org/concern/media/000398470?locale=en (2021).
62. Bour, R. & Maran, J. Une Nouvelle espèce de *Pelusios* de Côte d'ivoire (Reptilia, Chelonii, Pelomedusidae). *Manouria* **6**, 24–43 (2003).
63. Pérez-García, A. A taxonomic revision of the cenomanian bothremydid turtle *Algorachelus Parva* from Israel and morphological variation within its genus. *Palaeontologia Electronica*. **28**, 1–15 (2025).
64. De Broin, F. Sur La présence d'une tortue, *Pelusios sinuatus* (A. Smith) Au Villafranchien inférieur du Tchad. *Bull. De la. Société géologique De France*. **11**, 909–916 (1969).
65. Bramble, D. M. Emydid shell kinesis: biomechanics and evolution. *Copeia* 707–727, (1974). https://doi.org/10.2307/1442685 (1974).
66. Mlynarski, M. & Testudines *Handbuch der Palaoherpetologie* (1976).
67. Bramble, D. M., Hutchison, H. J. & Legler, J. M. Kinosternid shell kinesis: structure, function and evolution. *Copeia* 456–475, (1984). https://doi.org/10.2307/1445203 (1984).
68. Murelaga, X. et al. Amphibians and reptiles from the early miocene of the Bardenas Reales of Navarre (Ebro Basin, Iberian Peninsula). *Geobios* **35**, 347–365 (2002).
69. Joyce, W. G. & Bourque, J. R. A review of the fossil record of turtles of the clade *Pan-Kinosternoidea*. *Bull. Peabody Mus. Nat. Hist.* **57**, 57–95 (2016).
70. Joyce, W. G. & Claude, J. An alternative interpretation of the paleogene turtle *Cardichelyon rogerwoodi* as a hinged kinosternoid. *J. Paleontol.* **94**, 1–11. https://doi.org/10.1017/jpa.2019.92 (2020).
71. Joyce, W. G. Phylogenetic relationships of mesozoic turtles. *Bull. Peabody Mus. Nat. Hist.* **48**, 1–102 (2007).
72. Shah, R. V. *The mechanisms of carapacial and plastral hinges in chelonians*. (1960).

73. Cordero, G. A., Quinteros, K. & Janzen, F. J. Delayed trait development and the convergent evolution of shell kinesis in turtles. *Proc. R. Soc. B* **285**, 20181585. https://doi.org/10.1098/rspb.2018.1585 (2018).
74. Prokop, H. Breeding of the endemic Turkana mud turtle, Pelusios broadleyi Bour, 1986. *Radiata* **19**, 2–27 (2010).
75. Witte, G. F. d. *Amphibiens et reptiles. Exploration Hydrobiologique du Lac Tanganyika (1946–1947)*. Vol. 3(3) 1–22 (1952).
76. Gibbons, J. W. Variation in growth rates in three populations of the painted turtle, *Chrysemys picta*. *Herpetologica* **23**, 296–303 (1967).
77. Hewitt, J. Some new forms of batrachians and reptiles from South Africa. *Records Albany Museum*. **4**, 283–357 (1935).
78. Ferreira, G. S., Rincón, A. D., Solórzano, A. & Langer, M. C. The last marine pelomedusoids (Testudines:Pleurodira): a new species of *Bairdemys* and the paleoecology of the stereogenyina. *PeerJ* **3**, e1063. https://doi.org/10.7717/peerj.1063 (2015).
79. Mitchell, B. A naturalist in Nyasaland. *Nyasal. Agricultural Q. J.* **6**, 1–47 (1946).
80. Luiselli, L. et al. A comparative analysis of the diets of Pelusios turtles across Africa. *Diversity* **13**, 165 (2021).
81. Hailemichael, M. *The Pliocene Environment of Hadar, Ethiopia: a Comparative Isotopic Study of Paleosol Carbonates and Lacustrine Mollusk Shells of the Hadar Formation and of Modern Analogs* (Case Western Reserve University, 2000).
82. Stephens, P. R. & Wiens, J. J. Bridging the gap between community ecology and historical biogeography: niche conservatism and community structure in emydid turtles. *Mol. Ecol.* **18**, 4664–4679. https://doi.org/10.1111/j.1365-294X.2009.04378.x (2009).
83. Rodrigues, J. F. M., Villalobos, F., Iverson, J. B. & Diniz-Filho, J. A. F. Climatic niche evolution in turtles is characterized by phylogenetic conservatism for both aquatic and terrestrial species. *J. Evol. Biol.* **32**, 66–75 (2020).
84. Hermanson, G. & Evers, S. W. Shell constraints on evolutionary body size–Limb size allometry can explain morphological conservatism in the turtle body plan. *Ecol. Evol.* **14**, e70504 (2024).
85. Bonnefille, R., Potts, R., Chalié, F., Jolly, D. & Peyron, O. High-resolution vegetation and climate change associated with pliocene australopithecus afarensis. *Proc. Acad. Nat. Sci.* **101**, 12125–12129 (2004).
86. Bonnefille, R., Vincens, A. & Buchet, G. Palynology, stratigraphy and palaeoenvironment of a pliocene hominid site (2.9–3.3 M.Y.) at Hadar, Ethiopia. *Palaeogeogr., Palaeoclimatol. Palaeoecol.* **60**, 249–281 (1987).
87. Paquet, H. *Evolution géochimique Des minéraux Argileux Dans Les altérations Et Les Sols Des Climats méditerranéens Tropicaux a Saisons contrastées* Vol. 30 (Persée-Portail des revues scientifiques en SHS, 1970).
88. Yemane, T. *Stratigraphy and Sedimentology of the Hadar formation, Afar, Ethiopia* (Iowa State University, 1997).
89. Peypouquet, J., Carbonel, P., Taieb, M., Tiercelin, J. & Perinet, G. 277–285 (The University of Houston Press Houston, (1983).
90. Hay, R. L. in *In Background To Evolution in Africa*. 221–228 (eds Bishop, W. W. & Clark, J. D.) (University of Chicago Press, 1979).
91. Loveridge, A. & Peters, J. L. *Scientific Results of an Expedition To Rain Forest Regions in Eastern Africa: Reptiles* (Museum of Comparative Zoölogy, 1936).
92. Behrensmeyer, A. K. Paleoenvironmental context of the pliocene AL 333 first family hominin locality, Hadar Formation, Ethiopia. *Geol. Soc. Am. Special Papers*. **446**, 203–214 (2008).
93. Johanson, D. & Wong, K. *Lucy's legacy: the quest for human origins*Crown,. (2010).
94. Aronson, J. & Taieb, M. Geology and paleogeography of the Hadar hominid site, Ethiopia. *Hominid Sites: their Geologic Settings*, 165–195 (1981).
95. Reed, K. E. Paleoecological patterns at the Hadar hominin site, Afar regional State, Ethiopia. *J. Hum. Evol.* **54**, 743–768 (2008).
96. Njau, J. K. & Blumenschine, R. J. A diagnosis of crocodile feeding traces on larger mammal bone, with fossil examples from the Plio-Pleistocene Olduvai Basin, Tanzania. *J. Hum. Evol.* **50**, 142–162 (2006).
97. Selvaggio, M. M. & Wilder, J. Identifying the involvement of multiple carnivore taxa with archaeological bone assemblages. *J. Archaeol. Sci.* **28**, 465–470 (2001).
98. Drumheller, S. K. & Brochu, C. A. A diagnosis of *Alligator mississippiensis* bite marks with comparisons to existing crocodylian datasets. *Ichnos* **21**, 131–146 (2014).
99. Drumheller, S. K. & Brochu, C. A. Phylogenetic taphonomy: a statistical and phylogenetic approach for exploring taphonomic patterns in the fossil record using crocodylians. *Palaios* **31**, 463–478 (2016).
100. Milàn, J. et al. Crocodylian-chelonian carnivory: bite traces of Dwarf caiman, *Paleosuchus palpebrosus*, in red-eared slider, *Trachemys scripta*, carapaces. *Crocodile Tracks Traces Albuquerque: New. Mexico Museum Nat. History Sci. Bull.* **51**, 195–199 (2010).
101. Drumheller, S. K., D'Amore, D. C. & Njau, J. K. Taphonomic approaches to bite-mark analyses in the fossil record and applications to archosaurian paleobiology. *Ruling Reptiles: Crocodylian Biology Archosaur Paleobiology*, 161 (2023).
102. Carpenter, K. & Lindsey, D. The dentary of brachychampsa Montana Gilmore (Alligatorinae; Crocodylidae), a late cretaceous turtle-eating alligator. *J. Paleontol.* **54**, 1213–1217 (1980).
103. Erickson, B. R. Chelonivorous habits of the paleocene crocodile *Leidyosuchus formidabilis*. *Sci. Publications Sci. Museum Minn.* **5**, 1–7 (1984).
104. de la Fuente, M. S. Two new pleurodiran turtles from the Portezuelo formation (Upper Cretaceous) of Northern Patagonia, Argentina. *J. Paleontol.* **77**, 559–575 (2003).
105. Tichy, G. & Karl, H. V. The structure of fossil teeth of chelonophagous crocodiles (Diapsida: Crocodylia). *Studia Geologica Salmanticensia*, 115–124 (2004).
106. Mead, J. I. et al. Plio-Pleistocene *Crocodylus* (Crocodylia) from Southwestern Costa Rica. *Stud. Neotropical Fauna Environ.* **41**, 1–7 (2006).
107. Steadman, D. W. et al. Exceptionally well preserved late Quaternary plant and vertebrate fossils from a blue hole on Abaco, The Bahamas. *Proc. Natl. Acad. Sci.* **104**, 19897–19902 (2007).
108. Lehman, T. M. & Wick, S. L. *Chupacabrachelys complexus*, n. gen. n. sp. (Testudines: Bothremydidae), Ffrom the Aguja formation (Campanian) of West Texas. *J. Vertebr. Paleontol.* **30**, 1709–1725. https://doi.org/10.1080/02724634.2010.520782 (2010).
109. Noto, C. R., Main, D. J. & Drumheller, S. K. Feeding traces and paleobiology of a cretaceous (Cenomanian) crocodyliform: example from the Woodbine formation of Texas. *Palaios* **27**, 105–115. https://doi.org/10.2110/palo.2011.p11-052r (2012).
110. Hastings, A. K., Bloch, J. I. & Jaramillo, C. A. A new blunt-snouted dyrosaurid, *Anthracosuchus balrogus* gen. Et sp. nov. (Crocodylomorpha, Mesoeucrocodylia), from the palaeocene of Colombia. *Hist. Biol.* **27**, 998–1020 (2015).
111. Scheyer, T. M. et al. Trophic interactions between larger crocodylians and giant tortoises on Aldabra Atoll, Western Indian Ocean, during the late pleistocene. *R. Soc. open. Sci.* **5**, 171800 (2018).
112. Gônet, J., Rozada, L., Bourgeais, R. & Allain, R. Taphonomic study of a pleurosternid turtle shell from the early cretaceous of Angeac-Charente, Southwest France. *Lethaia* **52**, 232–243. https://doi.org/10.1111/let.12309 (2019).
113. Peters, C. R. & Blumenschine, R. J. Landscape perspectives on possible land use patterns for early pleistocene hominids in the Olduvai Basin, Tanzania. *J. Hum. Evol.* **29**, 321–362 (1995).
114. Peters, C. & Blumenschine, R. Landscape perspectives on possible land use patterns for early pleistocene hominids in the Olduvai Basin, tanzania: part II, expanding the landscape models. *Kaupia* **6**, 175–221 (1996).
115. Archer, W., Braun, D. R., Harris, J. W., McCoy, J. T. & Richmond, B. G. Early pleistocene aquatic resource use in the Turkana basin. *J. Hum. Evol.* **77**, 74–87 (2014).
116. Braun, D. R. et al. Early hominin diet included diverse terrestrial and aquatic animals 1.95 Ma in East Turkana, Kenya. *Proc. Natl. Acad. Sci.* **107**, 10002–10007 (2010).
117. Leakey, L. S. A new fossil skull from Olduvai. *Nature* **184**, 491–493 (1959).
118. Stewart, K. M. Early hominid utilisation of fish resources and implications for seasonality and behaviour. *J. Hum. Evol.* **27**, 229–245 (1994).

119. Steele, E. T. A unique hominin menu dated to 1.95 million years ago. *Proc. Natl. Acad. Sci.* **107**, 10771–10772 (2010).
120. Laurin, M., de Queiroz, K., Cantino, P., Cellinese, N. & Olmstead, R. The PhyloCode, type, ranks, and monophyly: a response to Pickett. *Cladistics* **21**, 605–607. https://doi.org/10.1111/j.1096-0031.2005.00090.x (2005).
121. Rasband, W. S. (U. S. National Institutes of Health, Bethesda, MD, USA, 1997–2016).
122. Adobe Creative Cloud [Computer software] (2025).
123. Laurent, R. F. *Contribution a l'herpetologie de la region des grands lacs de l'Afrique centrale: I. Généralités. II. Cheloniens. III. Ophidiens*. (1956).
124. Schweigger, A. F. *Enumeratio Plantarum Horti Botanici Regiomontani* (Typis Academicis, 1812).
125. Bour, R. Une Nouvelle espèce de *Pelusios* du Gabon (reptilia, Chelonii, pelomedusidae). *Manouria* **8**, 1–32 (2000).

Acknowledgements

We thank the Ethiopian Heritage Authority for allowing us to access the fossils in their care. We also could not have done the research without the help of the staff of the National Museum of Ethiopia and especially Sahle Melaku for assistance with the collections. We are grateful to Blade Redae for help in identifying crocodile bite marks and navigating the Hadar fossil collection. We are also appreciative of the team members of the International Afar Research Expedition (IARE) and Hadar Research Project (HRP) for their multiple year efforts to collect the fossils that were included in this study.

Author contributions

B.A. performed morphological descriptions, taxonomic comparisons, and manuscript writing. C.J.C., K.E.R., and D.R.F contributed to discussions and manuscript editing. B.A. created figures except Figure 1, which was provided by C.J.C.

Declarations

Competing interests

The authors declare no competing interests.

Additional information

Supplementary Information The online version contains supplementary material available at https://doi.org/10.1038/s41598-025-24655-8.

Correspondence and requests for materials should be addressed to B.A.